Environmental Challenges 19 (2025) 101118

Contents lists available at ScienceDirect

Environmental Challenges

journal homepage: www.elsevier.com/locate/envc

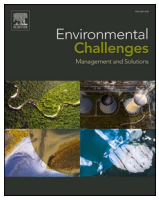

Refining land cover classification and change detection for urban water management using comparative machine learning approach

Douraied Guizani [a,b,*], János Tamás [a,b], Dávid Pásztor [a,b], Attila Nagy [a,b]

[a] Institute of Water and Environmental Management, Faculty of Agricultural and Food Sciences and Environmental Management, University of Debrecen, 146B Böszörményi str., 4032 Debrecen, Hungary
[b] National Laboratory for Water Science and Water Safety, Institute of Water and Environmental Management, Faculty of Agricultural and Food Sciences and Environmental Management, University of Debrecen, 146B Böszörményi str., 4032 Debrecen, Hungary

ARTICLE INFO

Keywords:
Land cover classification
Urban water balance
Machine learning
Remote sensing
Google Earth engine
Change detection
Debrecen
Hungary

ABSTRACT

Accurate land cover (LC) maps are essential for urban water balance modeling, particularly in rapidly urbanizing cities like Debrecen, Hungary, where industrial expansion has intensified since 2019. However, LC classification remains challenging due to limited studies evaluating the optimal combination of classifiers and satellite data. This study builds upon previous research by introducing a comparative analysis of three machine learning classifiers—Support Vector Machine (SVM), Maximum Likelihood Classification (MLC), and Random Forest (RF)—in LC classification using Sentinel-2 and Landsat 8 imagery from 2018, 2020, and 2022.

Results show that SVM on Sentinel-2 achieved the highest accuracy (F1 score: 0.84 ± 0.11, overall accuracy: 88 ± 2.1 %, kappa: 0.84 ± 0.03) with the lowest total disagreement values (D% = 12.6 in 2020, 13.1 in 2022). Consequently, SVM with Sentinel-2 was selected for LC change detection, employing trajectory analysis to assess urban development dynamics. The quantity gain component accounted for 5 % of the study area, representing net urban expansion, while the exchange component (10 %) indicated bidirectional shifts between developed and non-developed classes. Given Debrecen's rapid industrialization and the lack of a robust LC classification strategy for hydrological applications, this research refines LC change detection methods. It improves water balance calculations by LC type, strengthening the hydrological framework. By demonstrating the value of satellite imagery and GIS in monitoring urbanization, the findings support future urban water balance assessments, sustainable planning, and resource management, providing local authorities with a robust tool to adapt spatial strategies to an evolving landscape.

Introduction

Urbanization is a global process with long-term environmental consequences, particularly in terms of water resource management (Kintu et al., 2019). Expanding urban areas and replacing natural surfaces with asphalt and concrete abruptly change the Earth's surface characteristics (Njoku and Tenenbaum, 2022). This phenomenon is termed as LC change, and it has drastically changed the water balance of a city by disrupting normal runoff, infiltration, and evapotranspiration rates within an urbanizing watershed (Bueno-Suárez and Coq-Huelva, 2020). LC classification which is defined as the science of classifying and characterizing such surface features, is crucial to identify and overcome these challenges of urbanzation (Shi and Li, 2021). The satellite images also enable scientists to monitor the development of cities and their effects on water resources; vital data for monitoring environmental conditions and resource management. (Mudereri et al., 2023; Al-Bilbisi, 2019). The observation of trends in LC over time enables decision-makers to select the most appropriate method of land utilization, namely urban planning, agriculture, or conservation (Munthali et al., 2019). LC classification, besides, permits environmental modification like deforestation and desertification as very valuable input data for ecological conservation and management of land resources for sustainable use (Zhao et al., 2023).

Urbanization alters the landscape and creates problems in water resources management; hence, there is an all greater need to understand the LC of the Earth in urban areas (Caldwell et al., 2012). Runoff generation, evapotranspiration rates, and infiltration patterns change significantly whenever cities start growing and impervious surfaces

* Corresponding author at: University of Debrecen, 146B Böszörményi str., 4032, Debrecen, Hungary.
E-mail address: douraid.guizany@agr.unideb.hu (D. Guizani).

https://doi.org/10.1016/j.envc.2025.101118
Received 16 December 2024; Received in revised form 19 February 2025; Accepted 4 March 2025
Available online 5 March 2025

increase (EPA, 2023). This eventually affects the water balance in the entire city. In this respect, developing an efficient water management strategy for rapidly industrialized cities depends completely on accurate and updated LC information (Mengistu et al., 2022; Banjara et al., 2024).

Remote sensing (RS) satellite data are among the most valuable sources when up-to-date LC classification needs to be obtained, while big Earth Observation (EO) data sets are constantly used to obtain information on LC (Nagy et al., 2007, 2009, 2013; Maus et al, 2019). For instance, using SITS (Satellite Image Time Series) enhances a more rational comprehension of landscape and natural phenomena such as deforestation, greenhouse gas emission, and agricultural development as described by Petitjean et al., 2012. The LC classification highly depends on the satellite images availed through satellites such as Sentinel-2 and Landsat 8 (Jamshid et al., 2013; Jensen, 2000). These satellites capture Earth's surface in multiple wavelengths, providing information about infrastructure monitoring, vegetation, and water (Deng et al., 2019; Drusch et al., 2012). This spectral information is then analyzed by scientists to classify the different LC types (Navin et al., 2020). RS technology, especially from satellites, is very instrumental in the efficient monitoring of LC, Urban Planning, and Ecosystem and Biodiversity Health over large areas without extensive fieldwork, which can be very time-consuming and costly (Skidmore et al., 2021).

In supervised LC classification, the most important elements are training samples, classifiers, and supplemental datasets (Johnson, 2015). However, with the help of modern tools (like ArcGIS Pro and Google Earth Engine), we can create LC maps with more accuracy by utilizing various LC classification algorithms. In this paper, three algorithms, SVM, RF, and MLC, are applied for LC classification using satellite imagery. All these algorithms have their advantages given accuracy and interpretability. SVM excels in dealing with complex datasets and producing high accuracy because it can separate classes in high-dimensional spaces; RF offers robust performance with a lower risk of overfitting; and MLC, in particular, is appreciated for its probabilistic approach, as it assumes a normal distribution of the input data, hence being rather easy to implement and understand (Basheer et al., 2022; Talukdar et al., 2020; Adugna et al., 2022).

In our previous study (Guizani et al., 2024), we analysed the hydrological consequence of LC change in Debrecen, Hungary, a city experiencing rapid urbanization and industrial development. Our research focused on estimating infiltration, evapotranspiration, and runoff for the year 2019 to quantify the city's water balance, relying on a single classification method (MLC) and Landsat-8 imagery. However, accurately mapping LC remains challenging due to the lack of studies and methodologies focused on this region, particularly regarding multi-temporal analysis.

The innovation of this study lies in its comparative approach, which evaluates multiple machine learning classifiers (SVM, RF, and MLC) applied to both Sentinel-2 and Landsat 8 data over an extended period from 2018 to 2022. Contrary to other studies, which focused on a single classifier and one year, this research systematically assesses classification performance and improves LC change detection. This extended time frame allows for capturing LC changes that in Debrecen due to recent developments (Iváncsics and Kovács, 2021). The results offer a more robust LC mapping approach that enhances urban water balance modeling by minimizing classification errors. These results will not only inform future urban water balance assessments in Debrecen but also pave the way for improved urban planning and management strategies for rapidly urbanizing cities around the world.

Materials and methods

Description of the study area

Debrecen, Hungary's second-largest city, serves as the focal point of

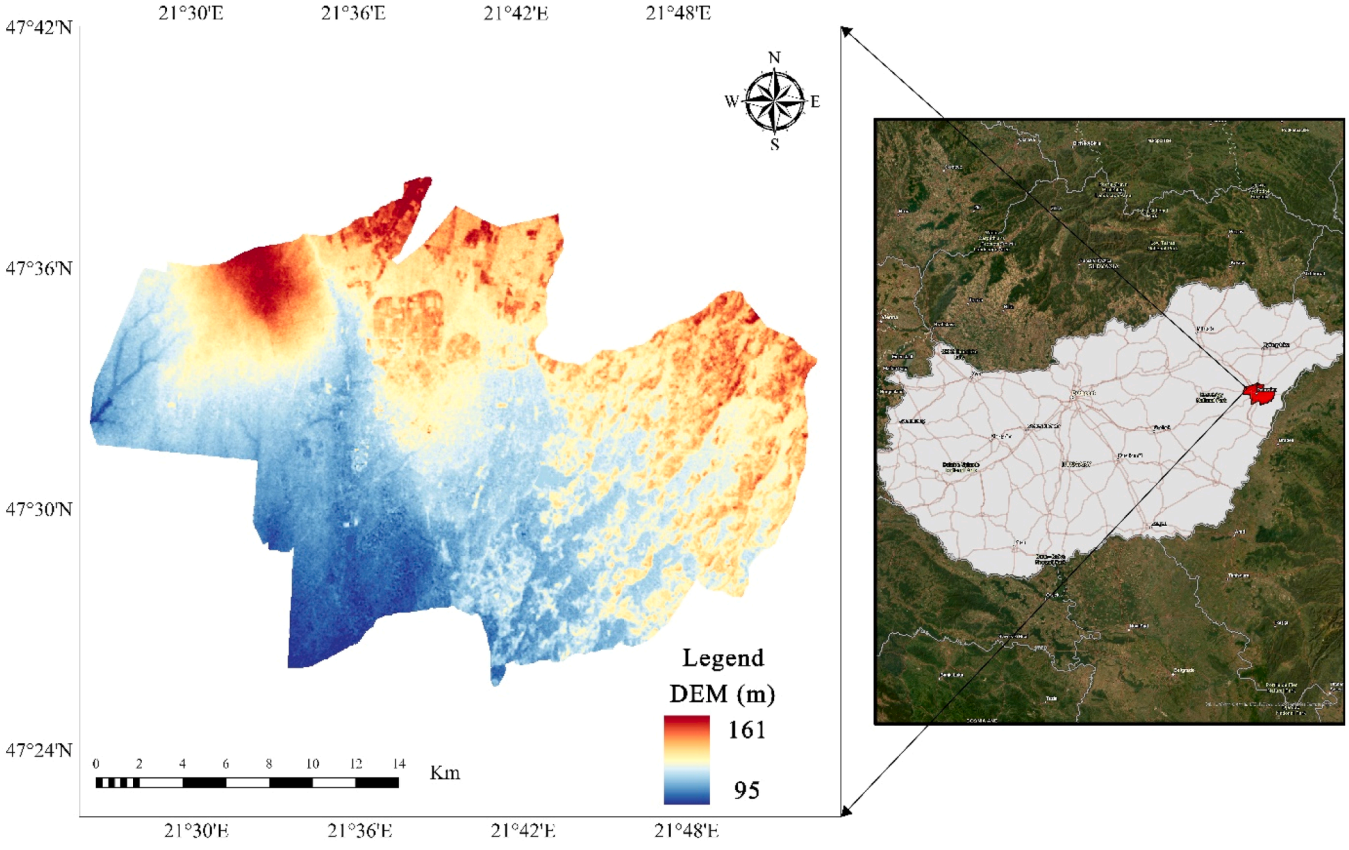

Fig. 1. Location of Debrecen within Hungary and digital elevation model (DEM).

this study (Kozma, 2009). Located in the eastern part of the country, Debrecen resides within Hajdú-Bihar County (Tamás et al., 2019) (see Fig. 1). Understanding Debrecen's LC and its transformation is crucial due to the city's rapidly increasing urbanization (Iváncsics and Kovács, 2021). This study aims to bridge the gap in existing research, as previous investigations haven't focused on LC changes in Debrecen.

Population: Debrecen boasts a population of over 200,000 residents, experiencing steady growth over the past decades. This population surge is a significant factor driving urban expansion and LC changes (STRATEGY 24, 2023).

LC: Debrecen's LC is likely undergoing a significant shift due to urban sprawl (Pénzes et al., 2023; Molnár and Kozma, 2018). As impervious surfaces, like buildings and roads, replace natural landscapes, infiltration patterns, evapotranspiration rates, and runoff generation are all significantly impacted (Dams et al., 2013). This, in turn, disrupts the city's overall water balance (Weng and Lu, 2008). Understanding the current LC and its transformation patterns will be essential for informed urban planning and sustainable development.

The city's water resources deserve mention as well. The Tisza River, one of Hungary's largest, flows near Debrecen, influencing the local hydrology (Lóczy et al., 2009). Additionally, Debrecen has different hydrological systems including natural water bodies, wetlands, and groundwater systems (Tony and Jorge, 2022). Understanding how these resources interrelate with the dynamic LC is crucial for sustainable water management (Banjara et al., 2024).

Water and Environmental Practices: Debrecen is located in a region that experiences periodic water shortages; therefore, effective management of this resource is very important. Research into the existing management practices of water and the potential sustainable use of water will be instrumental. Therefore, assessments of environmental practices related to waste management, pollution control, and development of green areas will be crucial to ensure the environmental health of Debrecen (STRATEGY 24, 2023).

Climate: Debrecen has a continental climate, indicating that summers are hot and winters are cold and snowy. Analysing LC changes and their possible effects on the urban environment will require an understanding of the climate (Szász, 2013).

Foreseen rapid urbanization: Debrecen, Hungary, is poised for a period of rapid urbanization (Iváncsics and Kovács, 2021). This trend can partly be attributed to a major increase in industrial development that occurred in 2019. The setting up of key players, such as a battery factory and BMW plant, has given impetus to the economy and led to a surge in new job opportunities (Hungarian Insider, 2022; Pénzes et al., 2023). This development, in terms of job creation, definitely had consequences for the urban environment of the city, such as in the advance of urbanized areas (Building Connections, 2024).The arrival of these industrial giants has attracted a new wave of residents seeking employment within the city. In this respect, urban spread in Debrecen will be maintained alongside this growing number of citizens. Such a trend presents both opportunities and challenges for city planners (Debrecen4u, 2024). This will demand new developments in housing, transportation networks, and public services to ensure both the transition of existing residents and that of the newcomers move smoothly (Debrecen4u, 2024 and STRATEGY 24, 2023).

Methodological framework for LC classification

Several traditional techniques exist which estimate LC changes at the global scale (Haque and Basak, 2017; Settembre et al., 2024). On the other hand, studies carried out in Debrecen city undergoing rapid industrialization have lacked an overall framework that analyze the changes in LC over time. Various studies on the rapid industrialization and urbanization of Debrecen have shown that a structured framework is necessary for efficiently tracking changes in LC over time. A few works center around suburbanization, urban sprawl, and the transformation of the outlying area by industrial growth. For example, within the PROSPERA project, a Strategic Urban Development Strategy (SUDS) was produced for Debrecen (PROSPERA, 2020) to balance sustainable practices and industrial expansion, especially within the periphery of cities. It also intends to enhance green infrastructure and climate resilience within the urban-suburban zones to reflect the increasing policy interest in the environment alongside growth in the urban areas (Hegedűs et al., 2023; PROSPERA, 2020). The impact of peripheral industrialization on LC in Debrecen is the subject of another study (Halder, 2022), which specifically links changes in the rural-urban transition zone to industrial expansion and foreign direct investment, especially in industries. In light of these structural shifts, there is a call for a comprehensive analysis framework that can integrate GIS and spatiotemporal data to capture both economic and environmental impacts.

The objective of this paper is to present a methodological framework that will analyze and compare the performance of different approaches for image classification to map LCs in Debrecen, Hungary. The framework addresses the limitations of previous research in the area, which predominantly used a single classifier with small datasets (PROSPERA, 2020; Hegedűs et al., 2023). The city of Debrecen is undergoing industrial development, which presents several challenges about the management of its water resources and the impact of changes in LC on the water balance. In our previous study (Guizani et al., 2024), we investigated these issues by employing only a single classifier and Landsat 8 data for a single year. This framework builds upon that previous work by incorporating: Comparative Analysis of Classification Methods: We move beyond a single classifier by comparing the performance of various algorithms within ArcGIS Pro. This allows us to identify the best-performing method for mapping Debrecen's dynamic LC.

- Spatiotemporal data collection: Sentinel 2 and Landsat 8 satellite images, collected between 2018 and 2022, and are used to leverage the advantage of geospatial big data. The multi-temporal technique allows for LC change analysis, in the urban region, between the specified years (Wiatkowska et al., 2021; Chaves et al., 2020).
- Pre-processing: Pre-processing of Sentinel-2 and Landsat-8 data attempts to account for atmospheric effects. For this reason, preprocessing is applied to the Level-1C product for Sentinel-2 (ESA, 2020) and the OLI-TIRS sensors for Landsat-8 (Gascon et al., 2017). Sentinel-2 has 13 spectral bands, while Landsat-8 has 11. The two datasets capture data with different levels of detail in spatial resolution and cover different wavelengths in multispectral resolution (Nguyen et al., 2024).
- Training data and Validation: The spectral separability test was performed to ensure that the training samples for different LC classes were distinct. The Transformed Divergence (T.D) and Jeffries Matusita (J.M) are two of the most common indices used to ascertain class separability, and therefore they were adopted at this validation stage both of the indices yield a score of between 0 and 2, and 2 is ideal separability while 0 is poor separability (Padma and Sanjeevi, 2014). ENVI software was utilized in the analysis because it provides advanced tools for checking spectral differences. To get an accurate classification result and improve training data quality, those classes having a separability value below a critical threshold (for instance, 1.9) were flagged for modification (Bruse and Fleer, 1998).
- Machine Learning-based Classification: Labeled points were overlaid on the corresponding Sentinel 2 and Landsat 8 imagery using the band combinations established in Basheer et al., 2022 and our previous research (Guizani et al., 2024); this combined spectral information served as an input for training the classification algorithms. In the classification process, data from Landsat-8 and Sentinel-2 were used for the years 2018, 2020, and 2022 with three widely recognized classifiers: RF, SVM, and MLC.
- Accuracy Assessment: Error matrix was generated by comparing the classified maps with medium to high-resolution imagery available in Google Earth Engine (GEE), specifically using Sentinel 2 (10 m

spatial resolution for visible (RGB) and near-infrared (NIR) bands), very high-resolution Google Earth images (https://earth.google.com/web), which provides sub-meter spatial resolution (from 0.3 m to 1 m, depending on the acquisition date and provider), and familiarity with the study area's characteristics (Wiatkowska et al., 2021; ISPRS, 2018). To ensure reliable LC maps, we employ a robust accuracy assessment strategy. Each classifier-dataset combination will be evaluated using the F1 score, OA, and kappa coefficient. The F1 score is particularly valuable as it considers both Precision and Recall accuracy, addressing limitations of the kappa coefficient. (Hand, 2012; Foody, 2020; Lyons et al., 2018). Additionally, Quantity Disagreement and Allocation Disagreement metrics (Pontius Jr and Millones, 2011) are incorporated to provide a more detailed evaluation of classification errors by distinguishing between class proportion errors and spatial misallocation errors, further enhancing the accuracy assessment.

- Interpretation: Maps and graphs will be used to effectively communicate and analyze the findings, allowing for clear comparisons between classification methods and datasets. Therefore data visualization plays a crucial role in comparing classification methods, as indicated by Kollert et al. (2021) and Kullenberg (2016).
- Change Detection: Change detection analysis was performed for the study period to diagnose LC dynamics in Debrecen. A statistical comparative analysis was carried out by quantifying the variations for each type of LC class.

The methodological framework details are presented in Fig. 2.

By implementing this multifaceted framework, we aim to achieve a more precise and insightful understanding of LC changes in Debrecen. This knowledge will be instrumental in monitoring LC changes, managing water resources, and supporting sustainable urban development in the city. Table 1 shows the major LC classes' scheme for the study area. We use six major classes, e.g., forest, surface water bodies, developed, bare ground, crop-covered areas, and grassland that represent the overall LC of Debrecen.

Data sources

This study utilizes multi-temporal satellite imagery from Landsat 8 Operational Land Imager (OLI) and Sentinel-2 Multi-Spectral Instrument (MSI) for the years 2018, 2020, and 2022. These datasets are selected due to their spectral capabilities and suitability for LC classification. The data was accessed through the USGS Earth Explorer and the Copernicus Open Access Hub.

Table 1
The major Name and description of LC classes for Debrecen.

Class Names	description
Forest	Forests are large areas (over half a hectare) dominated by tall trees (over 5 meters) with a dense overhead layer (more than 10 % covered). (FAO, 2000)
Developed	Highly built-up areas with more than 80 % of the ground covered by human-made structures like buildings, roads, and other paved surfaces. (Linda and Geir, 2021)
crop-covered area	These areas are fairly uniform, making them easy to spot in Landsat images. This is because they have a consistent color signature (spectral characteristics) and a simple, organized layout (regular field geometry). (Matthews et al., 2022)
Grassland	An area covered in mostly grass or similar plants, where animals can graze. (Schoenbaum et al., 2018)
Surface water bodies	Bodies of water are entirely surrounded by land. They're basically natural or man-made depressions that collect and hold water. (Williams et al., 2004; Monaghan et al., 2017)
bare ground	Any exposed earth that is not covered by plants, rocks, pavement, or other materials. (Liu et al., 2022)

Two satellite' images with different spatial resolutions are used in this study:

- **Landsat 8 OLI**: The Landsat satellite represents a fundamental component of the USGS National Land Imaging Program, delivering consistent, reliable, and comparable data since 1974. With a resolution of 30 m, OLI's multispectral images include nine bands: two in the short-infrared spectrum and five in the visible and near-infrared spectrum. Landsat 8 is ideal for change detection research across the years, it provides a long-term record with a 16-day repetition cycle (USGS, 2016; Nwagoum et al., 2023).
- **Sentinel 2 MSI**: provides a multispectral imaging system with a wide swath and higher spatial resolution (10 m). This supports Copernicus land monitoring research, including the observation of coastal regions and inland water cover, the analysis of vegetation, water bodies and water cover, and soil. There are thirteen spectral bands in Sentinel 2. (European Space Agency, 2024 and Acharki, 2022).
- Acquisition Parameters: This study uses images with cloud cover range between 0 % and 35 %, focusing on the growing season (June to September) when vegetation is most easily distinguished from other LC types, to train our machine learning algorithm to maximize vegetation recognition (Yan et al., 2023).

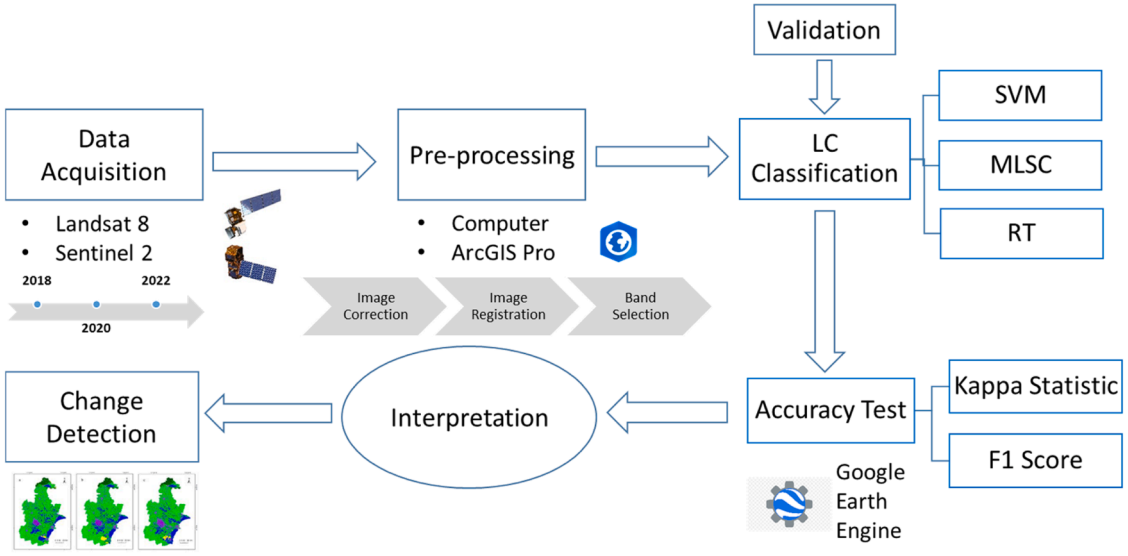

Fig. 2. Methodological framework details LC Classification and Change Detection using Sentinel 2, Landsat 8, and Machine Learning.

- Path-Row Information: The Worldwide Reference System (WRS) identification number of the downloaded scenes path-row was 186–27.
- Table 2 describes the sensor datasets and Acquisition time used in this study.

Sentinel-2 and Landsat-8 data were pre-processed to minimize atmospheric effects and improve classification accuracy. The steps included:

- Atmospheric Correction:
  - Landsat-8 OLI/TIRS: Atmospheric correction was conducted using the Apparent Reflectance tool in ArcGIS Pro. It scale the digital number (DN) values with regards to variables like sun elevation and sensor-specific parameters, which results in TOA reflectance values.
  - Sentinel-2 MSI: To minimise the impacts of atmospheric scattering, the Sen2Cor tool was employed to apply atmospheric correction as well as the of bottom-of-atmosphere (BOA) reflectance for the Sentinel-2 MSI.
- Cloud and Shadow Masking:
  - In Landsat 8, cloud cover masking is done by the Quality Assessment (QA) band in the Level-2 Surface Reflectance product. QA band contains details regarding the existence of clouds and shadows in very fine detail.
  - For Sentinel 2, cloud cover masking, was done using the Scene Classification Layer (SCL) included in the Level-1C data product. The SCL includes a per-pixel classification, which distinguishes, among other features, clouds, shadows, vegetation, and water. By delineating the pixels that were identified as clouds and shadows in the SCL, we effectively masked these regions so that they would not affect subsequent analyses.
- Geometric Correction:
  - Both datasets were geometrically aligned using ground control points and coordinate system standardization in ArcGIS Pro, ensuring spatial consistency across all images.
- Data Augmentation with Spectral Indices:
  - Normalized Difference Vegetation Index (NDVI): Calculated to highlight vegetated areas, aiding in distinguishing between different LC types.
  - Bare Soil Index (BSI): Computed to identify bare soil and fallow lands, enhancing the differentiation between agricultural and non-agricultural areas.

Training data and validation

The foundation for our LC classification lies in the training data (Shetty et al., 2021). We meticulously labeled sample points according to predefined LC classes, ensuring homogenous distribution across Debrecen. However, the number of samples for each class wasn't uniform. Instead, it reflected the proportional area each class occupies within the city. This approach ensures the training data accurately represents the true composition of Debrecen's LC. While the training data empowers the algorithms with the knowledge to recognize LC classes, the test data acts as an independent validation tool (Martinez-Sanchez et al., 2024). Once we have the reference datasets for every year between (2018, 2020, and 2022), we split them into two groups at random: 70 % for training and 30 % for validation (Aryal et al., 2023). The remaining 30 % of the labelled samples were reserved as test data, which serves as an independent validation set to evaluate the effectiveness of the trained algorithms (Amindin et al., 2024). A total of 3000 labeled points were selected for LC classification. These points were categorized into six LC classes. Out of these, 2100 points were used for change detection and classification, and 600 points were reserved for validation. We then used the band combination established by (Basheer et al 2022) and our previous work (Guizani et al., 2024) when projecting these labeled points onto the corresponding Landsat-8 and Sentinel-2 imagery. This combined spectral data is the main input used to train the classification models.

The multispectral response patterns of various LC categories were analyzed to identify spectral separability. Since spectral separability calculates the statistical separation between signatures, it establishes the OA of classification (Jackson and Adam, 2021). Jeffries Matusita's (J M) distance separability mesures and the transformed divergence (TD) index were used in the present study. Divergence (D) (Eq.1) is calculated using the variance-covariance matrices and mean of the data corresponding to feature classes (Kavzoglu and Mather, 2000).

Table 2
List of Sentinel-2 MSI and Landsat-8 OLI sensor datasets utilized in this research.

Satellite	Growth Season		Product Identifier	Acquisition time UTC
Landsat-8	2018	June	LC08_L1TP_186,027_20,180,620_20,200,831_02_T1	2018/06/20 09:20
		July	LC08_L1TP_186,027_20,180,706_20,200,831_02_T1	2018–07–06 09:20
		August	LC08_L1TP_186,027_20,180,823_20,200,831_02_T1	2018–08–23 09:20
		September	LC08_L1TP_186,027_20,180,908_20,200,831_02_T1	2018–09–08 09:20
	2020	June	LC08_L1TP_186,027_20,200,625_20,200,823_02_T1	2020–06–25 09:20
		July	LC08_L1TP_186,027_20,200,711_20,200,912_02_T1	2020–07–11 09:20
		August	LC08_L1TP_186,027_20,200,828_20,200,906_02_T1	2020–08–28 09:20
		September	LC08_L1TP_186,027_20,200,913_20,200,919_02_T1	2020–09–13 09:20
	2022	June	LC09_L1TP_186,027_20,220,623_20,230,410_02_T1	2022–06–23 09:20
		July	LC09_L1TP_186,027_20,220,725_20,230,406_02_T1	2022–07–25 09:20
		August	LC08_L1TP_186,027_20,220,818_20,220,824_02_T1	2022–08–18 09:21
		September	LC09_L1TP_186,027_20,220,911_20,230,329_02_T1	2022–09–11 09:20
Sentinel-2	2018	June	S2A_MSIL1C_20180619T094031_N0500_R036_T34TET_20230811T190137	2018–06–19 09:40
		July	S2B_MSIL1C_20180714T094029_N0500_R036_T34TET_20230820T012645	2018–07–14 09:40
		August	S2A_MSIL1C_20180828T094031_N0206_R036_T34TET_20180828T121318	2018–08–28 09:40
		September	S2B_MSIL1C_20180919T093029_N0500_R136_T34TET_20230820T025309	2018–09–19 09:30:
	2020	June	S2A_MSIL1C_20200628T094041_N0500_R036_T34TET_20230506T074207	2020–06–28 09:40:
		July	S2A_MSIL1C_20200705T093041_N0500_R136_T34TET_20230530T081333	2020–07–05 09:30
		August	S2B_MSIL1C_20200829T093039_N0209_R136_T34TET_20200829T105201	2020–08–29 09:30
		September	S2B_MSIL1C_20200921T094039_N0209_R036_T34TET_20200921T111126	2020–09–21 09:40
	2022	June	S2A_MSIL1C_20220628T094041_N0400_R036_T34TET_20220628T113959	2022–06–28 09:40
		July	S2B_MSIL1C_20220720T092559_N0400_R136_T34TET_20220720T101237	2022–07–20 09:25
		August	S2B_MSIL1C_20220819T092549_N0400_R136_T34TET_20220819T101112	2022–08–19 09:25
		September	S2B_MSIL1C_20220928T093039_N0400_R136_T34TET_20220928T101405	2022–09–28 09:30:

Source: ESA and NASA.

$$D_{ij} = \frac{1}{2} tr\left[\left(\sum j - \sum i\right)\left(\sum_{j}^{-1} - \sum_{i}^{-1}\right)\right] + \frac{1}{2} tr\left[\left(\sum_{j}^{-1} + \sum_{i}^{-1}\right)(\mu i - \mu j)(\mu i - \mu j)^{T}\right] \quad (1)$$

The TD (Eq.2) is employed to mitigate the impact of well-separated classes, which may lead to a rise in the average divergence value and a misleading divergence measure (Kavzoglu and Mather, 2000).

$$TD_{ij} = C\left[1 - e^{\frac{-Dij}{8}}\right] \quad (2)$$

Where Σi and Σj are the variance-covariance matrices of classes I and J, μi, and μj are the corresponding mean vectors, and c is a constant value that defines the range of TD values. The trace of a matrix is represented by tr, which means the total of the diagonal components of the matrix.

The following is a definition of the J-M distance (Eq.3) between distributions of two classes, ωi and ωj (Jia and Richards, 1999):

$$JMij^2 = 2\left(1 - e^{\wedge - Bij}\right) \quad (3)$$

Where $B_{ij\ is}$ the Bhattacharyya distance computed as (Kailath, 1967) (Eq.4):

$$Bij = \frac{1}{8}((\mu i - \mu j)^{T}\left(\frac{\sum j + \sum i}{2}\right)(\mu i - \mu j) + \frac{1}{2} ln\left(\frac{1}{2}\frac{|\sum j + \sum i|}{\sqrt{|\sum j|\,|\sum i|}}\right) \quad (4)$$

The mean reflectance of species I and J is represented by μi and μj, their covariance matrices by Σi and Σj, and the determinants of Σi and Σj are represented by |Σi| and |Σj|, respectively. T is the transposition function, and ln is the natural logarithm function.

As a general rule, classes are separable if the result is greater than 1.9, fairly separable if it is between 1.7 and 1.9, and not separable if it is below 1.7 (Jensen, J.2005).

Machine learning based classification

The power of machine learning classifiers was utilized to create the best-performing LC map of Debrecen, Hungary. These algorithms analyze training data containing labeled examples (e.g., pixels representing specific LC types) and learn to identify similar patterns in unseen data. Here, we'll explore three prominent classifiers employed in this study: SVM, MLC, and RF.

- Support Vector Machine (SVM)

  SVMs are powerful supervised learning models that excel at classification tasks and are used to resolve different problems related to

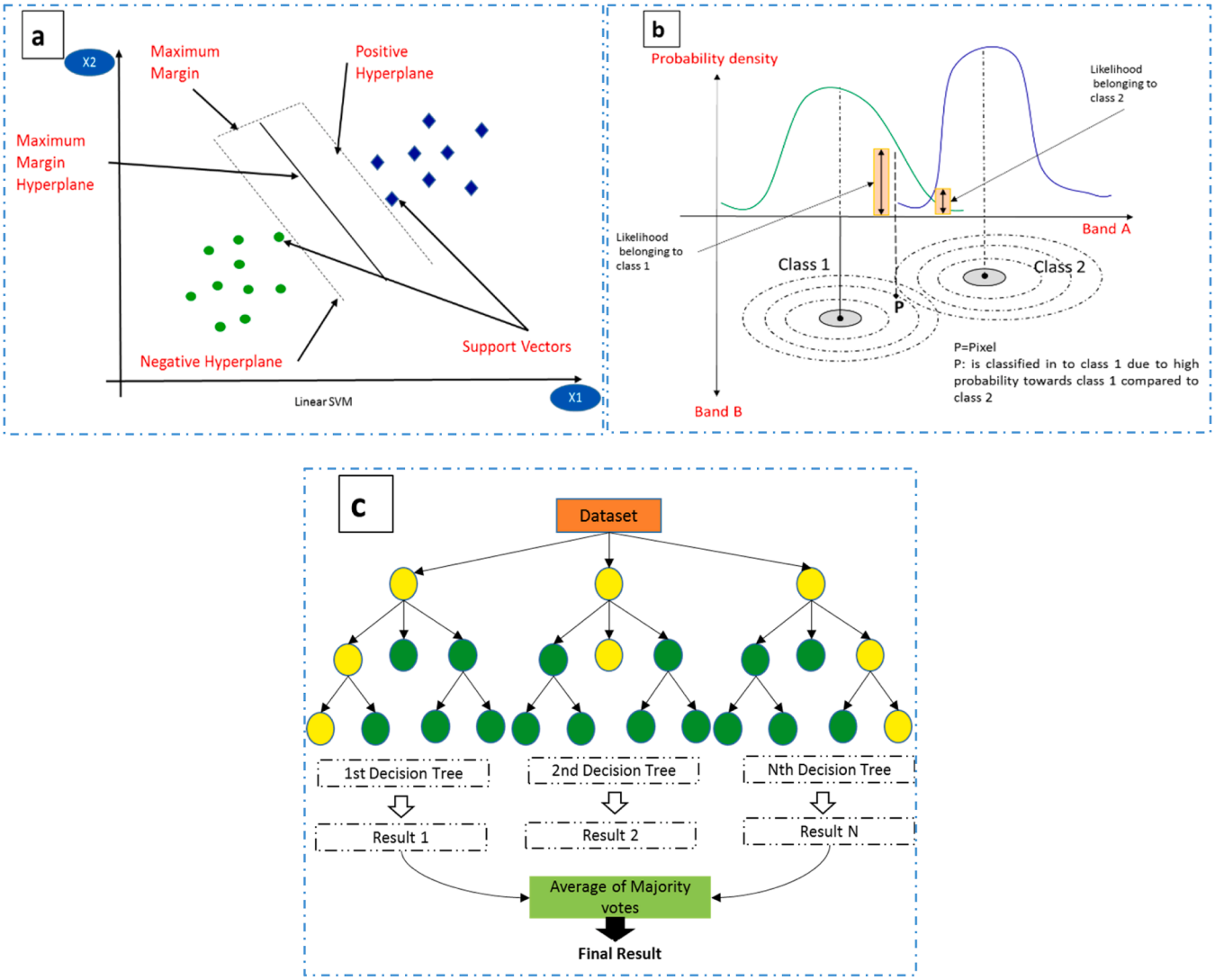

Fig. 3. A Concept of SVM Algorithm, b: Concept of MLC classification based on probability density. And c: Concept of RF Algorithm.

regression and classifications. They aim to find the optimal hyperplane (a decision boundary in high-dimensional space) that separates different LC classes with the maximum margin and less misclassified pixels from input datasets. This margin refers to the distance between the hyperplane and the closest training data points (support vectors) (Talukdar et al., 2020; Deilmai et al., 2014) (Fig. 3a).

Imagine a dataset with two LC classes: forest and water. An SVM seeks the hyperplane that best divides these classes while maximizing the distance between the hyperplane and the forest and water data points (support vectors). (Abbas et al., 2020).

For SVM, a radial basis function (RBF) kernel was used, with a gamma parameter of 0.1 and a regularization parameter (C) of 10, determined through cross-validation (Singh et al., 2019)

- Maximum Likelihood Classification (MLC)

MLC is a statistical classifier. It is presumed that each LC class follows a probability distribution in the feature space. MLC assigns a data point to the most likely class based on the statistical properties of the training data for each class. It is a supervised classification method based on the Byes theorem (Fig. 3b). (Deilmai et al., 2014; Norovsuren et al., 2019).

The MLC was implemented using a Bayesian approach with equal prior probabilities for all LC classes. These parameter settings were optimized to achieve the highest classification accuracy while maintaining computational efficiency (Cui Z et al., 2016).

- Random Forest (RF)

RF is a machine-learning method that combines the predictions of numerous decision trees (Breiman, 2001). Every tree is trained on a randomly selected subset of features and data points and creates a diverse "forest" of decision trees) (Fig. 3c). During classification, a new data point is passed through all trees, and the most frequent class prediction across all trees becomes the final output (Xie et al., 2019; Pal, 2005).

For the RF classifier, the number of trees was set to 500, and the number of predictors randomly selected at each split was set to the square root of the total number of input features. This configuration was chosen based on previous research and empirical tests to strike a balance between accuracy and computational efficiency (Lawrence et al., 2006).

Accuracy assessment

By applying the trained models on this test data through Google Earth high-resolution images combined with basic knowledge of the shape, color, and texture of the study area, we can assess their ability to classify LC (Dermosinoglou et al., 2024). Averaging the accuracy of test results per combination over the 2018–2022 period provides a robust indication of overall classification accuracy for the entire study duration.

High-quality reference data support provided by GEE enable strong accuracy estimations (Amindin et al., 2024). For the evaluation of the performance of each machine learning algorithm on Landsat-8 and Sentinel-2 imagery, important values such as Kappa index, OA, and F1 score were considered (Cohen et al., 1960; Lunetta et al., 1991 and Yonaba et al., 2021).The efficacy of different LC classifiers can vary significantly depending on the chosen method and specific field of research. Using various LC classifiers, prior research has shown slight to significant variations in classification accuracy (Qian et al., 2015; Sim et al., 2024). OA refers to the proportion of pixels of the testing data correctly classified and is used to assess the performance of any classifier (Moarrab et al., 2022). The accuracy of LC classification was evaluated using a multi-approach accuracy analysis, which consisted of Kappa coefficient, OA, and F1-score considering precision and recall accuracy per class (Naesset, 1996; Yonaba et al., 2021). While the OA and Kappa index are extremely popular, several studies revealed their limitations in their inability to consider random classification effects and class imbalance (Pontius and Millones, 2011; Pontius, 2022).To address these gaps, this study also employs the Quantity Disagreement and Allocation Disagreement metrics proposed by Pontius Jr and Millones (2011), which offer a more detailed evaluation of classification errors. These metrics distinguish between errors caused by incorrect number of classes (Quantity Disagreement) and errors caused by misallocation of pixels (Allocation Disagreement), overcoming the limitations of the Kappa statistic, which has been criticized for its dependence on prevalence and inability to differentiate between error categories.

- Overall Accuracy: represents the total classification accuracy. It is obtained by dividing the total number of correctly classified pixels by the total number of reference pixels. (Moarrab et al., 2021).
- Kappa Coefficient (k): It is one of the most widely applied methods of the accuracy assessment, it can be estimated easily from the confusion or error matrix (Lunetta et al., 1991). However, particularly in cases of imbalanced datasets, Kappa may not adequately indicate accuracy for individual classes and may be sensitive to the number of classes (Qian et al., 2015).
- F1-Score: This metric offers a more balanced view toward the performance of classification, entailing precision (the ratio of true positives among the predicted positive instances) and recall (the ratio of true positives identified from the ground truth) for every LC class. F1 score gives a better insight into performance, especially when some classes in the datasets are imbalanced (Sim et al., 2024).

OA (Eq. 5), Kappa (Eq. 6), and F1-Score (Eq. 8) are calculated using the metrics True Positive (TP), True Negative (TN), False Positive (FP), and False Negative (FN). TP (the instances correctly identified as positive), TN (the instances correctly identified as negative), FP (the instances incorrectly identified as positive), and FN (the instances incorrectly labeled as negative) are essential elements in evaluating the performance of classification models because by distinguishing between instances that were correctly and incorrectly classified (Sim et al., 2024).

$$OA = \frac{TP + TN}{TP + TN + FP + FN} \tag{5}$$

$$k = \frac{OA - Pe}{1 - Pe} \tag{6}$$

$$Pe = \left(\frac{TP + FN}{TP + FN + FP + TN} + \frac{TP + FP}{TP + FN + FP + TN}\right) * \left(\frac{FP + TN}{TP + FN + FP + TN} + \frac{FN + TN}{TP + FN + FP + TN}\right) \tag{7}$$

$$F1\ score = 2 * \frac{Precision * Recall}{Precision + Recall} \tag{8}$$

$$Precision = \frac{TP}{TP + FP} \tag{9}$$

$$Recall = \frac{TP}{TP + FN} \tag{10}$$

Pontius' quantity disagreement (Q) measures the differences in the proportion of area or quantity of each LC class. (Eq. 11) computes the overall quantity disagreement Q incorporating all J categories, while allocation disagreement (A) measures the differences in the spatial arrangement or misallocation of each LC class. (Eq. 12) gives the overall allocation disagreement A by summing the category-level allocation disagreements. Pontius' metrics were proposed to address some limitations of Cohen's kappa by explicitly considering the spatial allocation of LC classes, distinguishing between false positives and false negatives, and avoiding the assumption that disagreement occurs purely by chance. Eq. 13 shows how the total disagreement (D) is the sum of Q and A (Pontius & Millones, 2011).

$$Q = \frac{1}{2}\sum_{g=1}^{J} q_g; q_g = \left|\left(\sum_{i=1}^{J} P_{ig}\right) - \left(\sum_{j=1}^{J} P_{gj}\right)\right| \quad (11)$$

$$A = \frac{1}{2}\sum_{g=1}^{J} a_g; a_g = 2\min\left[\left(\sum_{i=1}^{J} P_{ig}\right) - P_{gg}, \left(\sum_{i=1}^{J} P_{gi}\right) - P_{gg}\right] \quad (12)$$

$$D = Q + A \quad (13)$$

Where q_g is the quantity disagreement for an arbitrary category g, which differs from the definition of q in Olofsson et al. (2014).

Stratified random sampling was used to develop a stratified dataset for accuracy assessment. Stratification ensures proper distribution of the sample across all LC classes in proportion, hence a more reliable evaluation of the result according to Stehman (2014).

Change detection: analysing urban expansion (2018–2022)

While the city of Debrecen is facing fast urbanization and industrialization (Pénzes et al., 2023), LC change detection studies specifically on this region are scarce (Szilassi, 2017; Kovács, 2011). Although LC changes may be detected from a variety of satellite imaging datasets using a variety of methodologies, the process can be complex and require careful consideration (Haque et al 2017; Settembre et al., 2024). Fortunately, the comparison of data from various satellites acquired on different dates provides a relatively simple but efficient method for LC change detection for any region (Boriah, 2010).

Our objective here Determine the quantitative increase in urban area size during the study period as a result of Industrialization. To achieve this, we leverage the best-performance LC maps created from the above section by using optimum satellite imagery and classification algorithm selected from our accuracy assessment. Given the complete comparability of the previous section on different classifiers and satellite imagery combinations, we adopt the approach that provided the best-performing LC maps for both 2018 and 2022. This ensures the highest confidence in the resulting change detection analysis. Specifically, the emphasis of this analysis will relate to the quantification and identification of those areas changing from non-urban to urban LC classes. The result will provide insight into the magnitude and spatial pattern of sprawl emanating from industrial development in Debrecen during the study period. The results would be presented with the use of maps and statistics on the magnitude and location of the urban expansion.

Trajectory analysis is a technique used to study LC change over multiple periods through the examination of the individual sequences of transitions that land categories go through. Using this approach, scientists can move beyond simple two-time-period comparisons and develop a more advanced understanding of the temporal patterns and dynamics of LC change.

We applied trajectory analysis in our study to examine the spatio-temporal dynamics of developed land in Debrecen between 2018 and 2022. Following the framework provided by Bilintoh et al. (2024), we categorized each pixel in our study area based on its LC status at each time point, deriving a trajectory that represents its specific sequence of transitions. This approach allowed us to classify pixels into various types of trajectory, such as "Gain without Alternation," "Loss without Alternation," "Stable Presence," "Stable Absence," and different forms of "Alternation."

By analyzing these trajectories, we could identify areas of continuous development, temporary change, and fluctuating LC states, providing a comprehensive overview of urban expansion and shrinking patterns. Our time series Trajectories R package performs the analysis and freely available at https://github.com/bilintoh/timeseriesTrajectories.

This is in line with the methodology used by Bilintoh et al. (2022) in comparing urban impervious surfaces, where trajectory analysis was utilized to distinguish long-term and short-term Land-use changes. By incorporating trajectory analysis, we aimed to capture the complexity of urban LC dynamics, offering insights into the processes driving change and informing sustainable urban planning strategies.

Results

Training data and validation

The spectral separability analysis, using the J-M and T-D indices, confirmed the high quality and effectiveness of the training data for both Landsat 8 (2018, 2020, and 2022) and Sentinel-2 (2018, 2020, and 2022) datasets. All LC class pairs showed very good spectral separability with J-M and T-D values much higher than the threshold of 1.9. This is indicative of the ability of the training data to capture the unique spectral characteristics of different classes of LC and hence has produced appropriate and reliable classification:

- ü All class pairs reached J-M index values higher than 1.9, meaning sufficient separability for a correct classification.
- ü The index of T-D showed a constant score of 2, representing total separability for the training data.

The results of the separability analysis show good separation between the spectral signatures of all LC class pairs. Results from the J M index and T D index always showed perfect results (>1.9), reflecting the strength of the training dataset in capturing the distinctive spectral features from one LC class to another. High values of separability range between 1.9 and 2, confirming the efficiency of the training data for classification.

Machine learning based LC classification

Table 3 presents a comparison of classification performance for the selected LC types. The analysis considers three classification methods (SVM, MLC, and RF) and two satellite image sources (Landsat 8 and Sentinel 2) across three years (2018, 2020, and 2022). Performance is evaluated using the F1 score for each LC type, OA, Kappa, and Pontius 'accuracy metrics.

The general results indicate that the combination of SVM and Sentinel 2 outperforms most other combinations. For instance, "the SVM classifier using Sentinel 2 images reached an OA of 90 % in 2020, while it had a corresponding value of 0.87 for Kappa. This performed even better for the classification performance of several LC types: forest, with an F1 score = 0.98 in 2020, developed areas, with an F1 score = 0.77, and grassland, with an F1 score = 0.92 in the same year.

A major focus of this analysis was on the selection of optimal combinations to identify urban areas. The outcome of the performed tests showed that, in detecting urban areas, the SVM classifier with Sentinel 2 imagery generally produced higher performance in all evaluation metrics. Take, for example, the F1 score for this combination: 0.88 for the class of the developed area in 2018 outperforms any other methods and image sources by a large margin. This indicates that SVM can efficiently extract the complex spatial and spectral patterns related to urban environments while Sentinel 2 with a very high spatial and spectral resolution will provide important information for accurate classification.

Although this research confirmed SVM and Sentinel 2 as the best-performing combination in the case of Debrecen city mapping. It should be considered that the optimal method may differ depending on different study objectives and regional characteristics (Noble, W. S. 2006; Cortes and Vapnik, 1995; Mountrakis et al., 2011). Further studies are required to consider and present additional classification algorithms and satellite sensors, together with different geographic contexts. The results of this study illustrate the possibility of generating accurate urban area maps for Debrecen, using SVM and Sentinel 2 data. These results are beneficial for several applications, such as Agricultural Management, urban planning, and environmental monitoring.

Fig. 4 presents the average F1 score of the LC class calculated over

Table 3
Accuracy assessment for all combinations of satellite imagery and machine learning classifiers.

satellite	classifiers	years	F1 score per LC types						OA %	Kappa	Q %	A %	D %
			forest	Developed	crop covered areas	grassland	surface water bodies	bare ground					
Landsat 8	SVM	2018	0.86	0.72	0.74	0.72	0.31	0.87	80	0.74	4.91	12.58	17.5
		2020	0. 96	0.74	0.63	0.88	0.66	0.7	83	0.78	11.8	5.9	17.7
		2022	0.92	0.75	0.75	0.83	1	0.82	85	0.8	7.05	8.33	15.3
	MLC	2018	0.83	0.6	0.78	0.8	0.53	0.78	78	0.72	7.8	10	17.8
		2020	0.95	0.44	0.52	0.67	0.9	0.72	71	0.63	4.48	15.22	19.7
		2022	0.96	0.8	0.7	0.79	0.66	0.75	83	0.77	3.9	10.6	14.5
	RF	2018	0.82	0.77	0.73	0.76	0.5	0.86	77	0.7	7.14	10.61	17.8
		2020	0.93	0.72	0.52	0.84	1	0.69	80	0.73	6.7	10.9	17.6
		2022	0.95	0.78	0.61	0.72	0.61	0.88	81	0.75	11.9	6.4	18.3
Sentinel 2	SVM	2018	0.87	0.88	0.86	0.89	0.57	0.86	85	0.81	3.69	9.43	13.1
		2020	0.98	0.77	0.88	0.92	0.66	0.75	90	0.87	5.6	7	12.6
		2022	0.94	0.75	0.87	0.9	0.73	0.93	89	0.85	4.2	11.1	15.3
	MLC	2018	0.93	0.45	0.66	0.78	0.85	0.9	80	0.75	5.5	14.5	20
		2020	0.95	0.79	0.93	0.87	0.66	0.75	85	0.8	4.33	9	13.3
		2022	0.92	0.67	0.73	0.81	0.73	0.8	83	0.79	8	13.3	21.3
	RF	2018	0.88	0.73	0.8	0.79	0.5	0.78	78	0.72	15	8.18	23.1
		2020	0.94	0.8	0.64	0.77	0.8	0.76	82	0.73	2.67	15.3	17.9
		2022	0.9	0.72	0.67	0.75	0.66	0.74	80	0.74	8	24	32

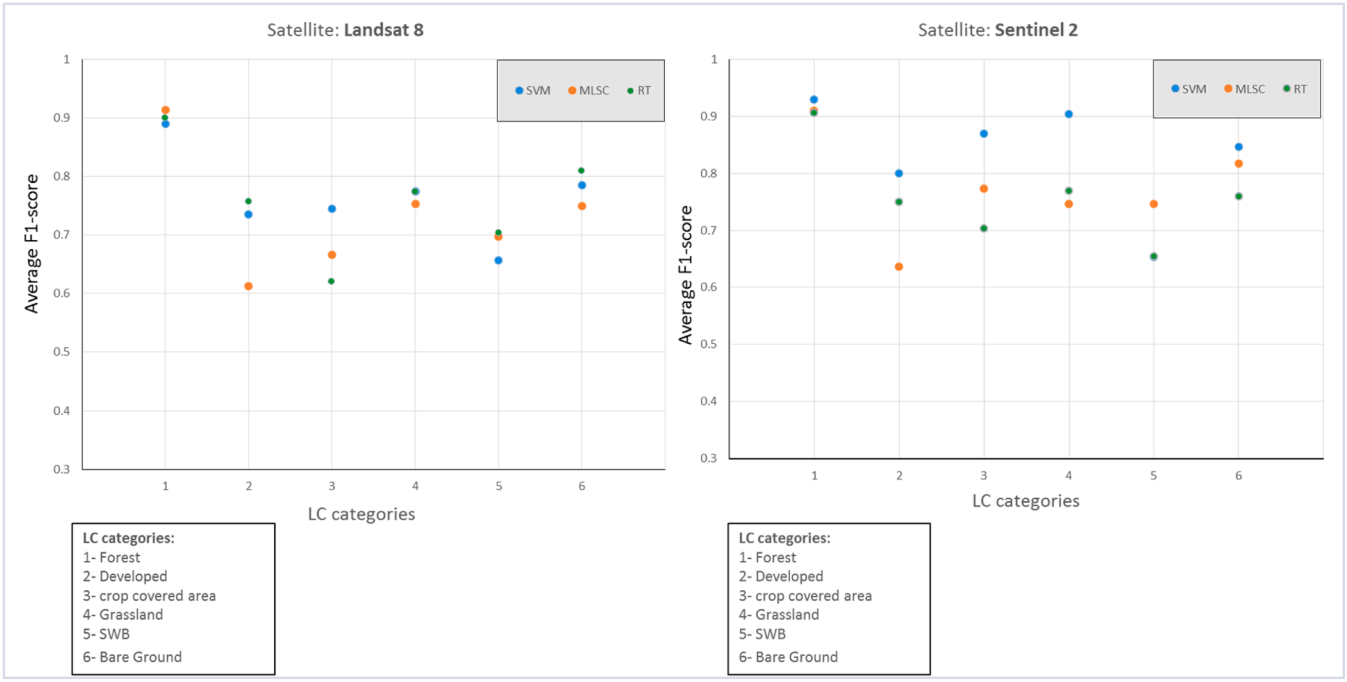

Fig. 4. Average F1-score distribution per categories.

the study period, evaluating the classification performance from different combinations of satellite imagery and classifiers. As illustrated in the figure, Sentinel 2 data have a higher F1 score with an SVM classifier for most of the classes, thus giving the best accuracy among all the other combinations.

The analysis of classification performance, as shown in Fig. 4, highlights key trends in the F1-scores across six LC classes. As an example, Sentinel-2 + SVM can achieve an average F1 score of about 0.93 for classifying the forest, which is the highest among all combinations. For crop-covered areas, the same combination gives an approximate average F1-score of 0.85, outperforming those derived from Landsat 8. Developed areas, as another critical LC class, are classified using Sentinel-2 + SVM, yielding an average F1 score of around 0.80 that outperforms other classifier-satellite combinations for the same LC class. These results then indicate how robust the Sentinel-2 data can get in the accurate capturing of complex LC patterns. Sentinel-2 consistently outperforms Landsat 8, demonstrating higher F1 scores due to its superior spatial and spectral resolution. For instance, the average F1-score of Landsat 8 + SVM is 0.87 for forest, while Sentinel-2 + SVM gets the value 0.93. Other classes, such as grassland, also show similar trends-for example, Sentinel-2 + SVM produces an F1-score of 0.90 for it, whereas Landsat 8 provides only 0.77.

Among classifiers, SVM shows the highest and most consistent performance for Debrecen. Achieving F1-scores above 0.85 for most LC categories, particularly excelling in Forest (0.93) and Bare Ground (0.846). Especially complemented with Sentinel-2 data, this combination allows SVM to realize the best F1-scores for the majority of LC classes since it can handle complex boundaries between classes (Pal and Mather, 2003; Zhao et al., 2023). In contrast, MLC and RF exhibit more variability, with MLC often trailing, especially for Developed and Crop-Covered Areas (e.g., Developed scores 0.636 with MLC compared to 0.8 with SVM for Sentinel-2). RF performs moderately well,

particularly for Grassland (e.g., 0.78 using Sentinel-2), and Developed areas (e.g., 0.75 using Sentinel-2), but struggles with Crop-Covered Areas (e.g., 0.703 for RF vs. 0.87 for SVM using Sentinel-2).

Consequently, Sentinel-2 combined with SVM is more likely to yield the best-performing and consistent results of the classification at the highest average F1 scores for the majority of LC classes. These results underscore the key role taken by high-resolution satellite imagery along with state-of-the-art classification algorithms in determining LC classification accuracy.

The classification performance analysis also considers disagreement metrics: Q %, A %, and D% to further evaluate the performance of different satellite-classifier combinations. These metrics provide additional insights into classification errors, distinguishing between misclassification due to incorrect class proportions and misclassification due to incorrect spatial placement.

Overall, Sentinel-2 data using SVM always exhibits the lowest disagreement values, confirming that it performs better than other classification methods. For instance, Sentinel-2 + SVM recorded the lowest total disagreement in 2020 (D% = 12.6), which is considerably lower than Landsat 8 + SVM (D% = 17.7) and other satellite-classifier combinations. This confirms that Sentinel-2′s spatial and spectral resolution significantly reduces classification errors.

Examining Q %, Sentinel-2 + SVM records some of the lowest values across different years, such as 5.6 % in 2020 and 4.2 % in 2022. In contrast, MLC shows a higher Q % for the same dataset, reaching 8 % in 2022, which suggests that for our study case, SVM provides a more precise estimation of class proportions. Similarly, Landsat 8 + SVM shows a higher Q % in 2020 (11.8 %) compared to Sentinel 2 + SVM (5.6 %), reinforcing the advantage of higher resolution Sentinel-2 data in reducing quantity-based misclassifications.

A % also highlights the excellence of Sentinel-2 + SVM in accurate class placement. For instance, this combination achieved an A % of 7 % in 2020, which is lower than Landsat 8 + SVM (8.33 %) and considerably better than other classifiers, such as MLC with Sentinel-2 (13.3 % in 2022). This suggests that SVM, when paired with Sentinel-2, is more effective in capturing the spatial distribution of LC classes, reducing allocation-based errors significantly.

The trends in Q, A, and D confirm that in our study SVM, particularly when applied to Sentinel-2 data, provides the most balanced and accurate classification. It consistently yields lower total disagreement values (D% = 12.6 in 2020, 13.1 in 2022), outperforming all other classifier-satellite combinations. These results further highlight the robustness of this approach in mapping urban and natural LC in Debrecen.

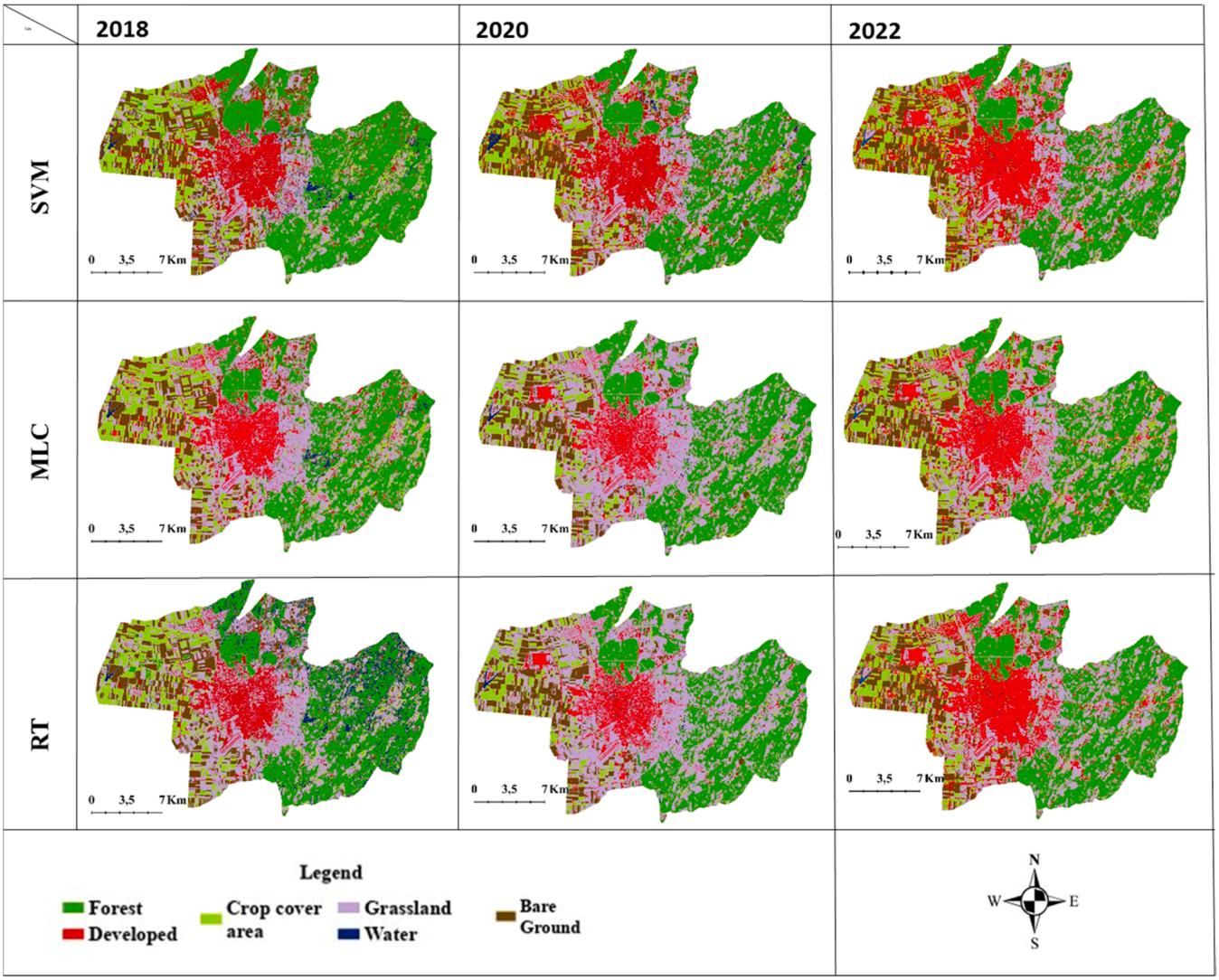

Fig. 5. LC classification maps of Landsat 8 images using SVM, MLC, and RF classifiers for the years 2018 to 2020 and 2022 in ArcGIS Pro.

Interpretation

LC classification of Landsat 8 imagery in ArcGIS pro

Using Landsat 8 imagery, the LC classification accuracy for 2018, 2020, and 2022 shows significant variations among classes and classifiers, as shown in Fig. 5.

Especially in 2018, the performance of the RF classifier was poor; frequently misclassifying forest areas as grassland or surface water bodies. This algorithm also frequently misclassified crop-covered areas as bare land or grassland in 2020. The MLC classifier in 2020, encountered challenges, most notably in distinguishing between developed areas, bare land, and grassland. Additionally, for both 2018 and 2022, the grassland was generally misclassified as a forest or crop-covered area.

In contrast, the SVM classifier demonstrated superior OA and F1 scores across all Landsat 8 images and years. Nevertheless, it had some issues, such as difficulty classifying grasslands and occasionally misidentified some urban areas for the year 2020.

Common among the erroneous classifications among both MLC and RF classifiers was vegetation being misclassified as grassland, more apparent in 2018 and 2020. This pattern might point to some spectral similarities among these LC types, which can hardly be differentiated.

The comparative analysis of L8-derived LC maps produced by different classifiers for the years 2018, 2020, and 2022 underlines large differences in the results of classification. Visual comparison of these maps within the same year but across different classifiers reveals these discrepancies. Furthermore, it is possible to observe from the visual comparison of the produced maps across the three years that LC changes took place over this period.

The findings emphasize the importance of carefully choosing appropriate classification algorithms and considerations of specific characteristics of the study area and target LC types should be taken into consideration in any RS-based LC mapping.

LC classification of sentinel 2 imagery in ArcGIS pro

The section presented here offers performance of three machine learning algorithms (SVM, MLC, and RF) for classifying LC using Sentinel-2 data. The study explored urban landscape growth from 2018 to 2022, and the strengths and weaknesses of the classifiers were assessed for every LC class.

Indeed, the SVM classifier performed better when compared with MLC and RF by yielding higher OA and F1 scores. For example, in 2020, an F1 score of 0.98 was obtained in the case of a forest for SVM, 0.77 in developed areas, 0.88 in crop-covered areas, 0.92 in grassland, 0.66 in surface water bodies, and 0.75 in bare ground. These values are higher compared to MLC and RF in general, reflecting the ability of SVM to

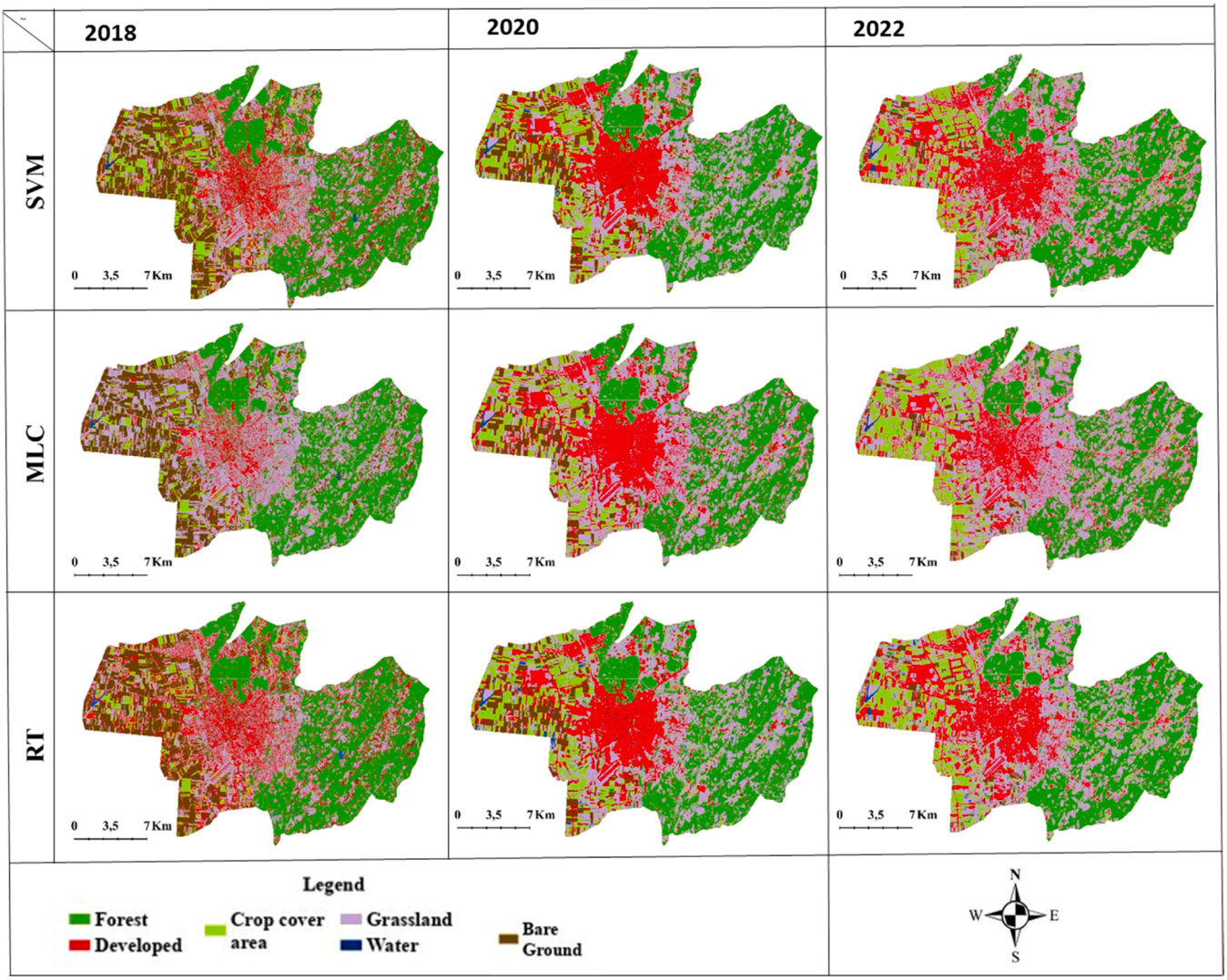

Fig. 6. Sentinel 2 image classification maps generated with ArcGIS Pro using SVM, MLC, and RF classifiers for 2018–2020 and 2022.

distinguish more accurately between different LC classes.

While SVM performed the best in general, all classifiers demonstrated their specific strengths and weaknesses regarding different LC types. For instance, MLC regularly had difficulty with developed areas, often misclassifying them as grassland or bare ground. In turn, RF had quite good performance for forest, developed, and bare ground but had problems with crop-covered areas and grassland classes. There was a significant increase observed in the built-up area for both 2018 and 2022 from the change computation of the LC maps produced by all classifiers (Fig. 6). The SVM classifier, being superior in identifying developed areas, gave the best-performing representation for urban expansion. The incorporation of Sentinel-2 imagery contributed to the OA of the LC classification. High spatial and spectral resolution, along with frequent revisit time, made Sentinel-2 very useful in capturing subtle changes in LCs, especially within urban areas. The availability of multiple years of Sentinel-2 imagery allowed accurate tracking of the development of urban areas and proper assessment of the performance of classifiers over time.

LC change detection

Fig. 7 below illustrates changes in LC categories for Debrecen City between 2018 and 2022. It is presented in terms of area (km^2), about different LC categories, namely barren ground, cropland, developed areas, forest, grassland, and surface water bodies.

The observed contraction of the surface water bodies by 0.89 km^2 from 2018 to 2022 in Debrecen fits well with the precipitation trends of the area. 2018 was quite rainy above the average; thus, it was a relatively wet year considering Central Europe. During this time, there was more water available and more surface water bodies were sustained due to heavy precipitation. However, from 2018 to 2020, an exceptionally long period of drought ensued, unparalleled in intensity and duration, marked by remarkable temperature anomalies and consistent precipitation deficits. The drought further worsened by 2022, and during the summer of 2022, it developed as one of the driest summers, with extreme soil moisture deficiencies and widespread classifications of droughts (Aalbers et al., 2023; Copernicus Climate Services, 2023).

The forested area in Debrecen has been drastically reduced to about 9.8 km^2 from the aforementioned time, basically due to compounded drought and urbanization. Vegetation was stressed with increased temperature and prolonged aridity, reducing the percentage of forest coverage. Such a trend has been further deteriorated by increased urbanization-earlier, natural habitat space had been transformed for infrastructure and industrial development. These dynamics reflect broader patterns observed throughout Central Europe, where the increased frequency of severe droughts tied to changing atmospheric circulations and climate variability have stressed ecosystems, with resultant changes in the form of land use (Gombos et al., 2023).

Other significant changes in LC included a loss of 67 km^2 in barren lands, coupled with an increase of 34 km^2 in grasslands, and an increase by 9.8 km^2 of crop-covered class. These trends may indicate large-scale LC transitions, likely due to expansion in agriculture and afforestation policies in response to changing environmental and socioeconomic pressures (STRATEGY 24, 2023). In comparison, this represents a growth in the developed area by approximately 33 km^2 and reflects more the preponderance of urban sprawl and infrastructural development. Such changes outline the dynamic interaction of climate-driven environmental stressors and human-induced land-use changes in shaping the landscape of Debrecen. All these shifts mark the nature of LC in Debrecen for the four years. The trends of growing built areas and declining woodland areas also indicate that Debrecen City's environmental environment is under increased human strain. Knowing this kind of change can ensure effective urban planning, environmental management, and sustainability in the resources of Debrecen.

Our analysis of LC changes reveals key insights into the dynamics of urban development, especially in regard to the perseverance, exchange, and alternation of developed areas. The Annual Change in the Presence of the developed area category (Fig. 8) decomposes LC transitions into three fundamental components: quantity gain, exchange, and alternation.

The quantity gain component, accounting for approximately 5 % of the study area, represents net urban expansion where land permanently transitioned into the developed category. The exchange component covers nearly 10 %, reflecting bidirectional shifts between developed and non-developed classes, indicating that certain areas remain in a state of flux rather than following a consistent urbanization trend. Most

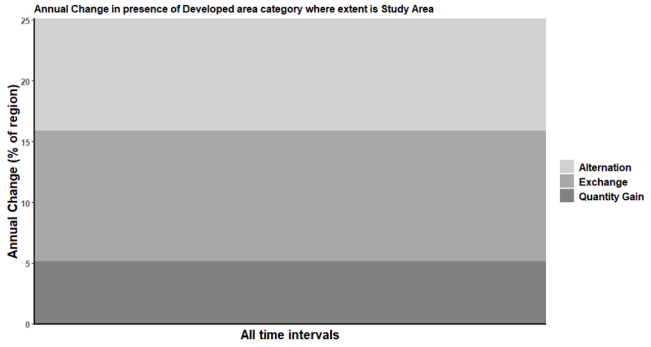

Fig. 8. Three components of change during the temporal extent expressed as the annual percentage of the unified size.

Fig. 7. Evaluation of LC changes in Debrecen City between 2018 and 2022.

notably, the alternation component, exceeding 10 %, highlights locations where developed land was intermittently classified across time intervals, suggesting significant land use competition and temporal instability. These findings align with Bilintoh et al. (2024), who emphasize that land-use alternation can be indicative of transient urban developments, ongoing construction projects, or classification inconsistencies in RS datasets.

A more detailed classification of these transitions is presented in the Developed Area Trajectories for Two Time Intervals (Fig. 9).

This plot categorizes LC changes into Loss without Alternation, Gain without Alternation, and Alternation. The Gain without Alternation category, representing over 10 % of the region, corresponds to areas that transitioned to developed land and remained stable, reflecting permanent urban expansion. In contrast, Loss without Alternation, covering nearly 5 %, represents areas where developed land was permanently lost, suggesting zoning modifications, redevelopment, or land-use reversion. Meanwhile, the Alternation categories (e.g., "Alternation Gain First" and "Alternation Loss First") collectively affect over 5 % of the study area, highlighting zones where classification oscillated, reinforcing the notion of land-use instability. These results corroborate findings by Bilintoh et al. (2022), which stress that trajectory-based urban land assessments are essential for distinguishing between temporary shifts and long-term urban transformation.

Collectively, these findings underscore the importance of integrating trajectory analysis into land change detection methodologies, as traditional classification-based approaches may misinterpret alternating land-use trends. The presence of substantial alternation in our study confirms the necessity of a multi-component framework to accurately assess urban development patterns ensuring a more refined understanding of long-term urbanization processes, land-use competition, and the stability of built environments in rapidly growing cities like Debrecen.

Discussion

Optimal LC classification combination

The selection of a classification algorithm depends on the nature of the data and the type of output expected. Though many studies point to robust SVM for high accuracy, RF for being able to manage data in high volume and complex form, and MLC for ease and computational efficiency of the technique, in our findings, SVM presented a better result compared to other approaches in urban LC classification (Noi and Kappas, 2018; Belgiu and Drăguţ, 2016; Qian et al., 2015).

Several important factors contribute to this superiority:

- Nonlinearity: The ability of SVM to deal with nonlinear relationships between features is very helpful in urban areas where LC classes often show complex spatial patterns and spectral characteristics (Pal and Mather, 2003; Zhao et al., 2023).
- Margin Maximization: The SVM algorithm aims to maximize the margin between classes. It thus delivers more robust and generalizable models. This is particularly useful in urban areas where class boundaries might be ambiguous or overlapping (Jamali, 2021; Chowdhury, 2024).
- Kernel Trick: The kernel trick allows the SVM to map data into a higher dimension, where it will be easy to obtain a linear separation. This is required to capture the complicated relationship between spectral bands and LC classes in urban environments (Pal and Mather, 2003; Zhao et al., 2023).

Combination of Sentinel-2 images with SVM proved particularly effective in our study. Due to the high spatial-spectral resolution, Sentinel-2 has the potential to provide a highly descriptive dataset for classifying LC classes in an urban environment with frequent revisit times. Because of their capability for processing complex data and nonlinear relationships, SVM can make full use of the information contained in Sentinel-2 imagery to generate an accurate classification map (Mohamed Abd, 2019; Chowdhury, 2024).

While our results are in agreement with several studies that

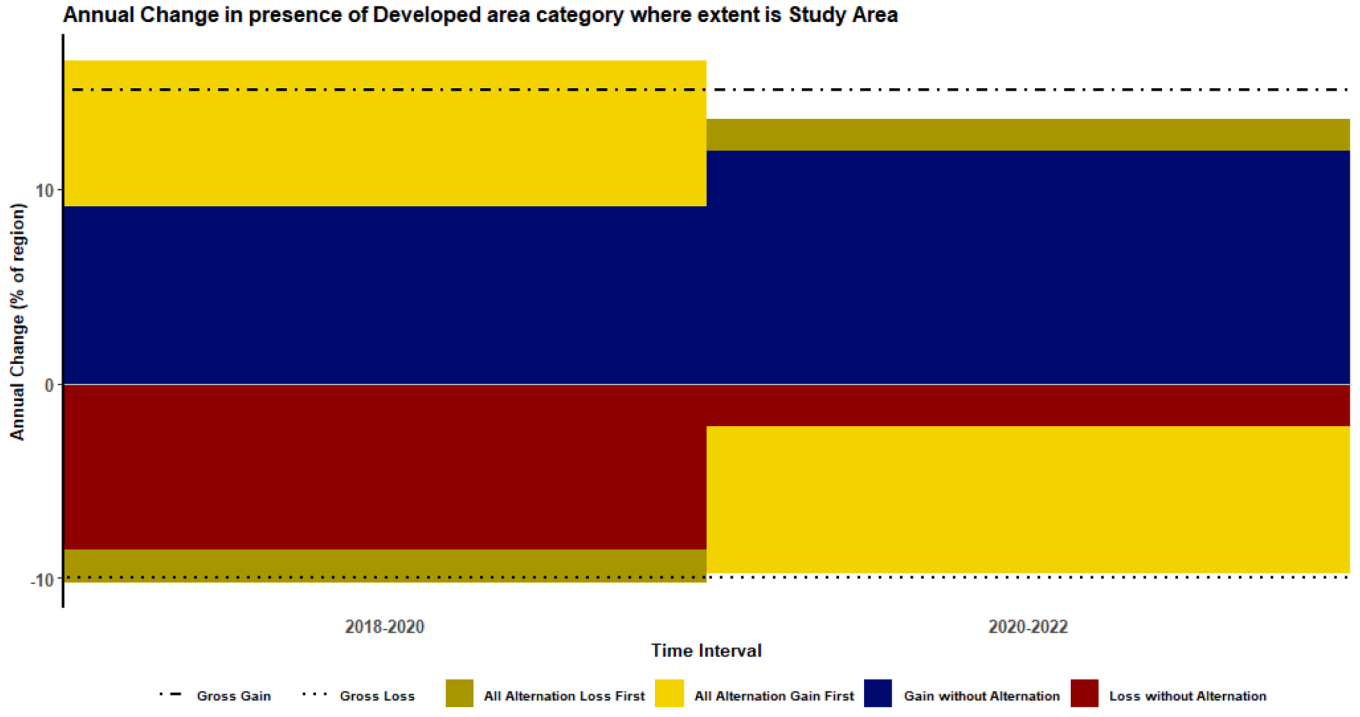

Fig. 9. Annual Gain and Loss for developed area category during two time interval.

identified SVM as the best classifier to map urban LC (Abbas et al., 2020; Deilmai et al., 2014), several other studies have identified either an RF or MLC classifier to perform better (Talukdar et al., 2020; Zhang et al., 2021; Basheer et al., 2022). Such discrepancies may be attributed to several factors:

- Characteristics of Data: Particular characteristics of the study area such as LC diversity, spatial distribution, and spectral variability may affect the performance of various classifiers (Adugna et al., 2022; Teodoro et al., 2024).
- Classifiers' objectives: The objectives of the study, such as the level of accuracy that is to be achieved or classes of interest, can also affect the choice of classifier (Zhang et al., 2021).
- Data Pre-processing: The pre-processing steps applied to the data, such as feature selection, normalization, and noise reduction, can significantly affect classification results (Alshdaifat et al., 2020).

RT may be preferable to large-scale LC mapping studies of natural ecosystems since these provide extensive data with similarly intricate spatial patterns (Breiman, L. 2001). Conversely, the MLC classifiers may be efficient for simple tasks and conditions in which computational resources are limited (Zakariyya et al., 2023).

In general, our study highlights the performance of SVM for urban LC classification, especially when integrated with Sentinel-2 imagery. The superior performance of SVM can be attributed to its ability to handle nonlinear relationships (Noble, 2006), maximize margins, and leverage the kernel trick (Cortes and Vapnik, 1995; Mountrakis et al., 2011). While other classifiers may be suitable for different study areas or objectives, our findings provide valuable insights into the optimal combination for urban LC mapping.

LC dynamics and changes

Clear trends of LC changes in Debrecen between 2018 and 2022, primarily due to urbanization and industrial expansion, as demonstrated by the analysis of Figs. 10 and 11. The largest alteration was in grasslands, where 28.89 km^2 were turned into developed areas. Bare ground (16.96 km^2) and crop-covered areas (12.21 km^2) came next. With the construction of new companies and industrial zones after 2019, the city's rapid growth especially about industrialization became more pronounced.

The conversion of grasslands and agricultural lands indicates that these areas, typically located on the outskirts of urban centers, were ideal for development due to their accessibility and lower economic value compared to forests. Industrialization, in particular, likely drove these conversions, as new factories required large, flat tracts of land for infrastructure.

The relatively low conversion of forest areas (4.17 km^2) and surface water bodies (0.44 km^2) suggests that environmental conservation measures are in place, or that these areas are less suitable for industrial or urban development. However, some minimal deforestation could still be linked to infrastructure expansion related to new factories.

The "No Change" category, accounting for 369 km^2, reflects that a substantial portion of Debrecen's land remained untouched. This indicates that, while urban sprawl has accelerated, particularly from 2019 onward due to industrial investments, there is still a significant portion of land under protection or not yet targeted for development.

Fig. 11 presents the trajectory analysis of developed areas over two-time intervals (2018–2020 and 2020–2022), offering insights into the spatiotemporal patterns of urban change. The classification highlights stable, expanding, contracting, and fluctuating developed areas, helping to distinguish permanent urbanization from temporary land-use transitions.

The results indicate that:

Stable developed areas (gray) dominate the urban core, confirming long-term urban permanence. New urban expansion (blue) is concentrated in suburban areas and along transportation corridors, reflecting ongoing infrastructure-driven growth.

Areas experiencing temporary urbanization (yellow and brown) are mainly located at the city's periphery, indicating fluctuations due to redevelopment or transitional land use.

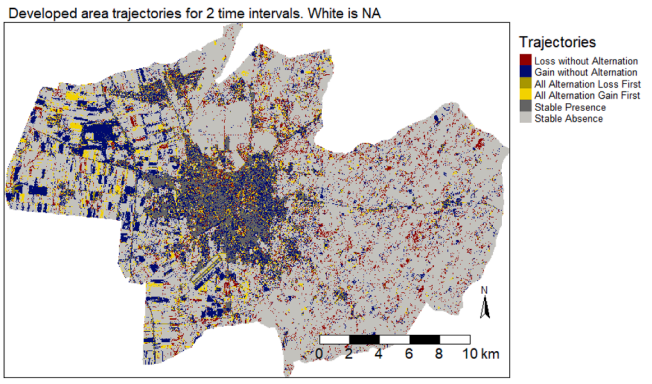

Fig. 11. Developed area Trajectories for two time intervals (2018–2022).

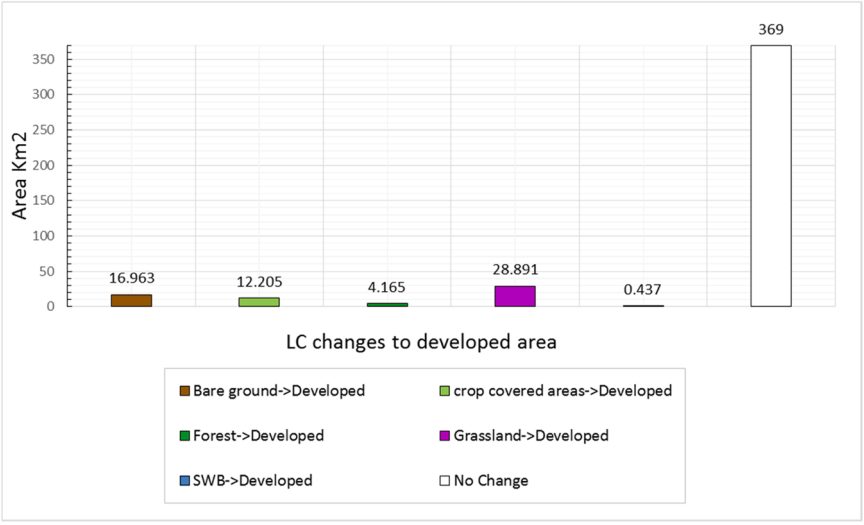

Fig. 10. Debrecen Urban Sprawl mapping based on LC changes between 2018 and 2022.

Land-use contraction (red) is observed in certain regions, suggesting reclassification or shifts in land use. These findings emphasize the dynamic nature of urbanization, where peripheral regions undergo continuous transformations while the core remains stable. The trajectory-based assessment provides a more detailed perspective on urban change, supporting urban planning strategies aimed at managing sustainable expansion and mitigating land-use instability.

Case Studies of LC Change Hotspots between 2018 and 2022

The spatial map (Fig. 12) shows that, mostly due to industrial growth beyond 2019, the majority of Debrecen's development is focused around already-existing metropolitan areas.

This expansion has primarily impacted grasslands and agricultural areas, pushing urban sprawl outward. However, the minimal changes in forest and water bodies suggest some level of environmental preservation, though continued expansion poses future risks. As Debrecen grows, it may face challenges such as loss of natural habitats, increased environmental degradation, and pressure on resources, making sustainable urban planning essential to balance development and conservation.

Fig. 13 presents a comparative analysis of LC changes between 2018 and 2022 in four distinct areas, utilizing the optimal combination of satellite imagery and classification techniques. By juxtaposing classified imagery with high-resolution aerial photographs derived from Google Earth, the figure offers a comprehensive overview of urban development intensity fluctuations.

The selected study areas represent a diverse spectrum of LC types to capture the multifaceted nature of urbanization. These include:

- BMW Industrial Complex: This site showcases rapid industrial expansion since its establishment in 2019, enabling the quantification of land transformation from green fields to industrial zones.
- JÓZSA Residential Area: As a residential development, this area provides insights into suburban growth patterns and the conversion of agricultural or green spaces into residential neighborhoods.
- Battery Production Industrial Park: This site is crucial for assessing the impact of emerging industrial sectors on land use, particularly focusing on the transformation of previously undeveloped or agricultural land.

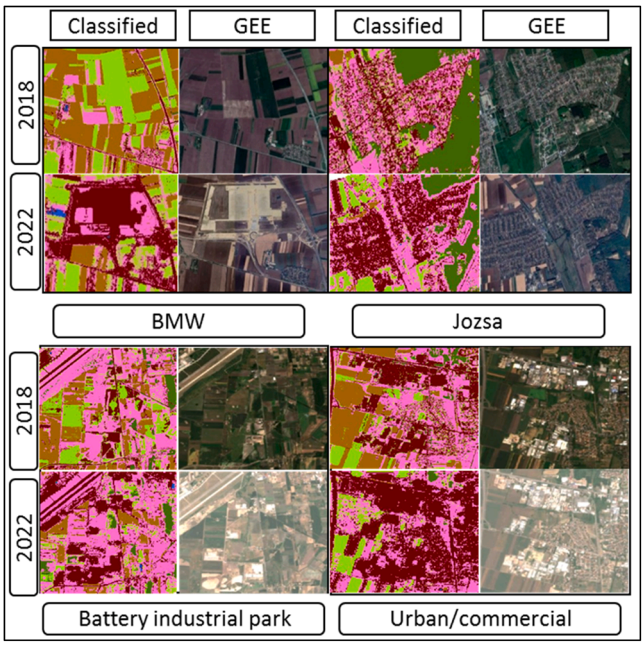

Fig. 13. four sample areas represent the change in urban development intensity between 2018 and 2022.

- Urban Commercial Area: By examining this area, the figure highlights changes in commercial LC, including the development of retail spaces, offices, and entertainment facilities.

This study aims to develop an improved basis for future urban water balance studies in Debrecen by determining the best combination of machine learning classifiers and satellite imagery for the generation of highly accurate LC maps with detailed data regarding each LC class that enhances their applicability for hydrological modeling. The refined LC information will, as future work, be integrated into the existing

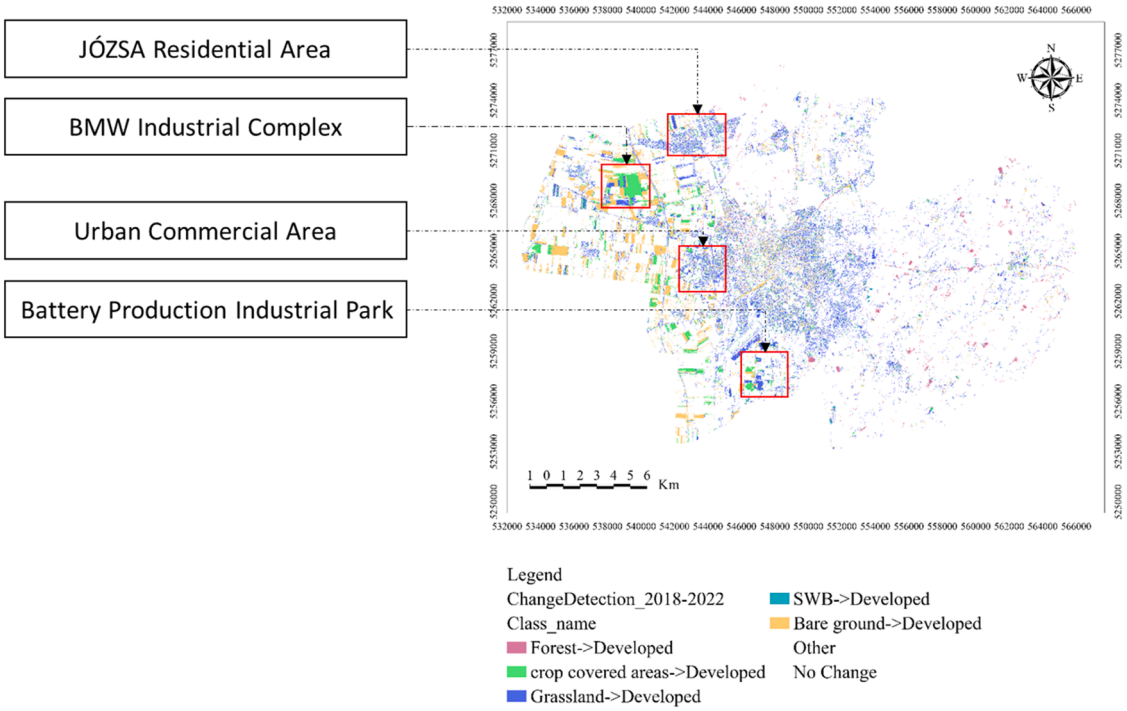

Fig. 12. Visualizing Urban Sprawl: LC Dynamics in Debrecen.

hydrological frameworks established in our previous study (Guizani et al., 2024) and permit more detailed infiltration, evapotranspiration, and runoff calculations. The integrated framework will be set up through high-resolution LC maps with our earlier methodology, which enables pixel-based calculations of hydrological parameters at the scale of Debrecen. Besides, LC change analysis during the study period is going to be carried out using the best-performing classification techniques to get a deeper view of the dynamics of urban development. By integrating these results with our previous works, we can work out an updated, accurate assessment tool of urban water balance, able to support informed decisions and sustainable urban planning.

In our previous study conducted for the year 2019, LC classification using the MLC method yielded an OA of 81.2 % and a kappa coefficient of 0.78. The F1 scores for specific LC classes were 0.70 for developed areas, 0.72 for bare ground, 0.66 for grasslands, and 0.60 for crop-covered areas. In contrast, the current study demonstrates improved classification performance over the study period (2018–2022) by employing Sentinel-2 imagery and the SVM classifier. The average OA for the 3 study years was 88.0±2.3 %, while the average kappa index reached 0.84±0.03, signifying enhanced reliability and accuracy. The results also indicated a substantial improvement in the F1 scores, with grasslands averaging 0.90, bare ground 0.85, developed areas 0.80, and crop-covered areas 0.85. This enhancement highlights the effectiveness of combining Sentinel-2 data with advanced classification algorithms such as SVM.

The improved classification outcomes provide a more reliable representation of LC dynamics in Debrecen. By integrating these improved LC maps into hydrological models developed in our previous study, we will be able to achieve more accurate and meaningful simulations of water resource management in the Debrecen urban area. The increased accuracy and robustness of the results reinforce the potential for using RS techniques and advanced classification methods in LC assessments to better support hydrological and urban planning efforts.

Conclusion

The present study develops LC classification and change detection methodologies for the city of Debrecen, Hungary, by fusing multi-satellite imagery sources such as Landsat-8 and Sentinel-2, using different machine learning classifiers over multiple years, namely RF, MLC, and SVM, in 2018, 2020, and 2022, correspondingly. Results show that SVM outperforms MLC and RF in terms of OA and F1 score, particularly when Sentinel-2 imagery is combined. A more accurate and comprehensive LC map that reflects Debrecen's dynamic urban growth and development can be updated thanks to this crucial improvement in the collection of more specific information on rapidly changing urban regions.

This study is an important step forward from our earlier work, which used a single classifier for LC classification and hydrological parameter integration using single-year Landsat-8 images. This approach provides a more dynamic view of urban evolution and can improve the accuracy of LC maps by integrating several years of data and comparative examination of various classifiers. Such improved LC maps can serve as input in hydrological models to provide a robust basis for an accurate assessment of the urban water balance that helps resolve rising issues in the management of water resources in a rapidly urbanizing city like Debrecen.

Moreover, LC changes analyzed in the period between 2018 and 2022 provide new insights into the spatial patterns and scope of Debrecen's urban expansion, highlighting the city's changing landscape due to increasing infrastructure development and urbanization. This highlights the importance of high-resolution, multi-temporal LC mapping for informed urban planning and water resource management, particularly in areas with limited historical data on LC change and rapid expansion.

The methodological developments discussed here create new avenues for future study, both in improving urban hydrological models and extending this approach to other rapidly urbanizing areas. Through the use of sophisticated satellite imagery and multi-temporal, multi-classifier techniques, this study lays the groundwork for more accurate and thorough evaluations of urban environments.

CRediT authorship contribution statement

Douraied Guizani: Writing – original draft, Visualization, Validation, Software, Methodology. **János Tamás:** Supervision, Funding acquisition, Formal analysis, Data curation. **Dávid Pásztor:** Methodology, Software, Writing – review & editing. **Attila Nagy:** Writing – review & editing, Writing – original draft, Supervision, Software, Resources, Project administration, Methodology, Conceptualization.

Declaration of competing interest

The authors declare that they have no known competing financial interests or personal relationships that could have appeared to influence the work reported in this paper.

Acknowledgment

The research presented in the article was carried out within the framework of the Széchenyi Plan Plus program with the support of the RRF 2.3.1 21 2022 00008 project.

Data availability

Data will be made available on request.

References

Abbas, Z., Jaber, H.S., 2020. Accuracy assessment of supervised classification methods for extraction land use maps using remote sensing and GIS techniques. IOP Confer. Ser. Mater. Sci. Eng. 745, 012166. https://doi.org/10.1088/1757-899X/745/1/012166.

Acharki, S., 2022. PlanetScope contributions compared to Sentinel-2, and Landsat-8 for LULC mapping. Remote Sens. Applic. Soc. Environ. 27, 100774. https://doi.org/10.1016/j.rsase.2022.100774.

Aalbers, E.E., van Meijgaard, E., Lenderink, G., de Vries, H., van den Hurk, B.J.J.M., 2023. The 2018 west-central European drought projected in a warmer climate: how much drier can it get? Nat. Hazards Earth Syst. Sci. 23, 1921–1946. https://doi.org/10.5194/nhess-23-1921-2023.

Al-Bilbisi, H., 2019. Spatial monitoring of urban expansion using satellite remote sensing images: a case study of Amman City. Jordan. Sustain. 11 (8), 2260. https://doi.org/10.3390/su11082260.

Adugna, T., Xu, W., Fan, J., 2022. Comparison of Random Forest and Support Vector Machine Classifiers for Regional Land Cover Mapping Using Coarse Resolution FY-3C Images. Remote Sens.. 14 (3), 574. https://doi.org/10.3390/rs14030574.

Aryal, J., Sitaula, C., Frery, A.C., 2023. Land use and land cover (LULC) performance modeling using machine learning algorithms: a case study of the city of Melbourne. Austr. Sci. Rep. 13 (1), 13510. https://doi.org/10.1038/s41598-023-40564-0.

Alshdaifat, E., Alshdaifat, D., Alsarhan, A., Fairouz, H., El-Salhi, S.M.F.S., 2020. The effect of preprocessing techniques. Appl. Numer. Features Classif. Algorithms' Performance. Data 6 (2), 11. https://doi.org/10.3390/data6020011.

Amindin, A., Siamian, N., Kariminejad, N., Clague, J.J., Pourghasemi, H.R., 2024. An integrated GEE and machine learning framework for detecting ecological stability under land use/land cover changes. Glob. Ecol. Conserv. 53, e03010. https://doi.org/10.1016/j.gecco.2024.e03010.

Basheer, S., Wang, X., Farooque, A.A., Nawaz, R.A., Liu, K., Adekanmbi, T., Liu, S., 2022. Comparison of land use land cover classifiers using different satellite imagery and machine learning techniques. Remote Sens. 14 (19), 4978. https://doi.org/10.3390/rs14194978.

Belgiu, M., Drăguţ, L., 2016. Random forest in remote sensing: a review of applications and future directions. ISPRS J. Photogr. Remote Sens. 114, 24–31. https://doi.org/10.1016/j.isprsjprs.2016.01.011.

Banjara, M., Bhusal, A., Ghimire, A.B., Kalra, A., 2024. Impact of land use and land cover change on hydrological processes in urban watersheds: analysis and forecasting for flood risk management. Geosciences. 14 (2), 40. https://doi.org/10.3390/geosciences14020040.

Breiman, L., 2001. Random forests. Mach. Learn. 45 (1), 5–32. https://doi.org/10.1023/A:1010933404324.

Bueno-Suárez, C., Coq-Huelva, D., 2020. Sustaining what is unsustainable: a review of urban sprawl and urban socio-environmental policies in North America and Western Europe. Sustainability. 12 (11), 4445. https://doi.org/10.3390/su12114445.

Building Connections, 2024. Debrecen Launches the Largest Urban Infrastructure Development Programme in Decades. Retrieved from. https://buildingconnections.eu/.
Boriah, S., 2010. Time Series Change detection: Algorithms for Land Cover Change (Doctoral Dissertation. University of Minnesota. Retrieved from. https://hdl.handle.net/11299/90706.
Bruse, M., Fleer, H., 1998. Simulating surface–plant–air interactions inside urban environments with a three dimensional numerical model. Environ. Modell. Softw. 13 (3-4), 373–384. https://doi.org/10.1016/S1364-8152(98)00042-5.
Bilintoh, E., Ali, M., Smith, D., 2024. Analyzing the Losses and Gains of a Land Category: Insights from the Total Operating Characteristic. Land. (Basel) 13 (8), 1177. https://doi.org/10.3390/land13081177.
Bilintoh, E., Adams, T., Zhang, X., 2022. Intensity Analysis to Study the Dynamics of Reforestation in the Rio Doce Water Basin. Brazil. Front. Remote Sens. 3, 873341. https://doi.org/10.3389/frsen.2022.873341.
Chowdhury, M.S., 2024. Comparison of accuracy and reliability of random forest, support vector machine, artificial neural network and maximum likelihood method in land use/cover classification of urban setting. Environ. Challenges 14, 100800. https://doi.org/10.1016/j.envc.2023.100800.
Copernicus Climate Change Service, 2023. European State of the Climate 2023. European Union. Retrieved from. https://climate.copernicus.eu/esotc/2023.
Chaves, E.D., Picoli, M.C.A., Sanches, I.D., 2020. Recent applications of Landsat 8/OLI and Sentinel-2/MSI for land use and land cover mapping: A systematic review. Remote Sens. (Basel) 12 (18), 3062. https://doi.org/10.3390/rs12183062.
Cohen, J.A., 1960. A coefficient of agreement for nominal scales. Educ. Psychol. Meas. 20 (1), 37–46. https://doi.org/10.1177/001316446002000104.
Caldwell, P.V., Sun, G., McNulty, S.G., Cohen, E.C., & Myers, M.J.A. (2012). Impacts of Impervious Cover, Water Withdrawals, and Climate Change on River Flows in the Conterminous U.S. Hydrology and Earth System Sciences, 16, 2839–2857. https://doi.org/10.5194/hessd-9-4263-2012.
Cortes, C., Vapnik, V., 1995. Support-Vector Networks. Mach. Learn. 20, 273–297. https://doi.org/10.1023/A:1022627411411.
Cui, Z., Ying, W., Gao, X., Li, J., Yu, Z., 2016. Multispectral image classification based on improved weighted MRF Bayesian. Neurocomputing. Volume 212, 75–87. https://doi.org/10.1016/j.neucom.2016.03.097.
Deilmai, B.R., Ahmad, B.B., Zabihi, H., 2014. Comparison of two classification methods (MLC and SVM) to extract land use and land cover in Johor Malaysia. IOP Conf. Ser.: Earth Environ. Sci. 20. https://doi.org/10.1088/1755-1315/20/1/012052. Article 012052.
Dermosinoglou, A., Petropoulos, G.P., 2024. Exploring long term Impervious Surface Areas (ISA) dynamics using Landsat imagery, Machine Learning and GEE: The case of Attica, Greece. Remote Sens. Applic. Soc. Environ. 36, 101338. https://doi.org/10.1016/j.rsase.2024.101338.
Debrecen4u, 2024. Huge Infrastructure Development in the Eastern part of Debrecen. Retrieved from. https://debrecen4u.hu/.
Deng, Z., Zhu, X., He, Q., Tang, L., 2019. Land use/land cover classification using time series Landsat 8 images in a heavily urbanized area. Adv. Space Res. 63 (7), 2144–2154. https://doi.org/10.1016/j.asr.2018.12.005.
Drusch, M., Del Bello, U., Carlier, S., Colin, O., 2012. Sentinel-2: ESA's optical high-resolution mission for GMES operational services. Remote Sens. Environ. 120, 25–36. https://doi.org/10.1016/j.rse.2011.11.026.
Dams, J., Dujardin, J., Reggers, R., Bashir, I., Canters, F., Batelaan, O., 2013. Mapping impervious surface change from remote sensing for hydrological modelling. J. Hydrol. 485, 84–95. https://doi.org/10.1016/j.jhydrol.2012.09.045.
European Space Agency, 2024. Sentinel-2 User Guide. Retrieved from. https://sentinel.esa.int/web/sentinel/user-guides/sentinel-2-msi/overview.
Environmental Protection Agency (EPA), 2023. Urbanization - Stormwater Runoff. Retrieved from. https://www.epa.gov.
ESA, 2020. Sentinel-2 Overview. https://sentinel.esa.int/web/sentinel/missions/sentinel-2/overview (Accessed on February 10, 2021).
Foody, G.M., 2020. Explaining the unsuitability of the kappa coefficient in the assessment and comparison of the accuracy of thematic maps obtained by image classification. Remote Sens. Environ. 239, 111630. https://doi.org/10.1016/j.rse.2019.111630.
FAO, 2000. On Definitions of Forest and Forest Change. Forest Resources Assessment Programme 2000. Forestry Dept., RomeItaly, p. 14. Working Paper 33Available online: https://www.fao.org/forestry/4036-0a4d4289d7a629dd821f1ce032a83596b.pdf.
Jackson, C.M., Adam, E., 2021. Machine learning classification of endangered tree species in a tropical submontane forest using WorldView-2 multispectral satellite imagery and imbalanced dataset. Remote Sens. 13 (24), 4970. https://doi.org/10.3390/rs13244970.
Jensen, J.R., 2005. Introductory digital image processing: A remote sensing perspective. In: Keith, C.C. (Ed.), Prentice Hall Series in Geographic Information Science, 4th ed., pp. 136–142. https://doi.org/10.1080/10106048709354084 Saddle River, NJ, USA.
Jensen, J.R., 2000. Introductory Digital Image processing: a Remote Sensing Perspective, 3rd ed. Prentice- Hall Inc, New Jersey.
Jamshid, T., Nasser, L., Mina, F., 2013. Satellite Image Classification Methods and Landsat 5TM Bands. Department of Computer Engineering EMU University, North Cyprus Famagusta. https://doi.org/10.48550/arXiv.1308.1801.
Jamali, A., 2021. Land use land cover mapping using advanced machine learning classifiers. Ekológia 40 (3). https://doi.org/10.2478/eko-2021-0031.
Johnson, B., 2015. Scale issues related to the accuracy assessment of land use/land cover maps produced using multi-resolution data: comments on "the improvement of land cover classification by thermal remote sensing. Remote Sens. 7 (10), 13436–13439. https://doi.org/10.3390/rs71013436.
Jia, X., Richards, J., 1999. Segmented principal components transformation for efficient hyperspectral remote-sensing image display and classification. Trans. Geosci. Remote Sen. 37, 25–27. https://doi.org/10.1109/36.739109.
Haque, M.I., Basak, R., 2017. Land cover change detection using GIS and remote sensing techniques: A spatio-temporal study on Tanguar Haor, Sunamganj, Bangladesh. Egypt. J. Remote Sens. Space Sci. 20 (2), 251–263. https://doi.org/10.1016/j.ejrs.2016.12.003.
Halder, S., 2022. Industrialization and the Transition of the Urban Fringe in Debrecen. University of Debrecen]. University of Debrecen Repository, Hungary [Master's thesisRetrieved from. https://dea.lib.unideb.hu.
Hegedűs, L.D., Túri, Z., Apáti, N., Pénzes, J., 2023. Analysis of the intra-urban suburbanization with GIS methods—The case of Debrecen since the 1980s. Folia Geographica 65 (1), 23–39.
Hungarian Insider, 2022. BMW Factory in Debrecen to Produce a Brand New Model from 2025. Retrieved from. https://hungarianinsider.com.
Hand, D.J., 2012. Assessing the performance of classification methods. Int. Statist. Rev. 80 (3), 400–414. https://doi.org/10.1111/j.1751-5823.2012.00183.x.
Iváncsics, V., & Kovács, K.F. (2021). Analyses of new artificial surfaces in the catchment area of 12 Hungarian middle-sized towns between 1990 and 2018. Land Use Policy, 109. https://doi.org/10.1016/j.landusepol.2021.105644.
ISPRS, 2018. Image classification & accuracy assessment using Landsat 8 and Sentinel 2A. The International archives of the photogrammetry. Remote Sens. Spatial Inf. Sci. XLII-3/W4, 17–20. https://isprs-archives.copernicus.org/articles/XLI-B8/1055/2016/isprs-archives-XLI-B8-1055-2016.pdf.
Guizani, D., Bódi, E.B., Tamás, J., Nagy, A., 2024. Enhancing water balance assessment in urban areas through high-resolution land cover mapping: Case study of Debrecen. Hungary. Environ. Challenges 15, 100906. https://doi.org/10.1016/j.envc.2024.100906.
Gombos, B., Nagy, Z., Hajdu, A., Nagy, J., 2023. Climate change in the Debrecen area in the last 50 years and its impact on maize production. IDŐJÁRÁS /Q. J. Hungarian Meteorol. Service 127 (4), 485–504. https://doi.org/10.28974/idojaras.2023.4.5. ISSN 0324-6329.
Gascon, F., Bouzinac, C., Thépaut, O., Jung, M., Francesconi, B., Louis, J., Gaudel-Vacaresse, A., 2017. Copernicus Sentinel-2A Calibration and Products Validation Status. Remote Sens. (Basel) 9 (6), 584. https://doi.org/10.3390/rs9060584.
Kavzoglu, T., Mather, P.M., 2000. Using feature selection techniques to produce smaller neural networks with better generalization capabilities. In: Proceedings of the IGARSS 2000. IEEE 2000 International Geoscience and Remote Sensing Symposium. Taking the Pulse of the Planet: The Role of Remote Sensing in Managing the Environment. Proceedings (Cat. No. 00CH37120), 7. Institute of Electrical and Electronics Engineers (IEEE), pp. 23–31. https://doi.org/10.1109/IGARSS.2000.860339.
Kailath, T., 1967. The Divergence and Bhattacharyya Distance Measures in Signal Selection. Trans. Commun. Technol. 15, 52–60. https://doi.org/10.1109/TCOM.1967.1089532.
Kintu, M., Shitenga, A., Shitenga, M., 2019. A literature review of impacts of urbanization on water resource management: A case study in South Africa. Int. J. Sci. Res. Public. 9 (6). https://doi.org/10.29322/IJSRP.9.06.2019.p9051.
Kollert, A., Bremer, M., Löw, M., Rutzinger, M., 2021. Exploring the potential of land surface phenology and seasonal cloud-free composites of one year of Sentinel-2 imagery for tree species mapping in a mountainous region. Int. J. Appl. Earth Observ. Geoinf. 94, 102208. https://doi.org/10.1016/j.jag.2020.102208.
Kullenberg, C., Kasperowski, D., 2016. What is citizen science? A scientometric meta-analysis. PLoS. One 11 (1), e0147152. https://doi.org/10.1371/journal.pone.0147152.
Kozma, G., 2009. Place marketing in Hungary: the case of Debrecen. Eur. Spatial Res. Policy 16 (1), 59–74. https://www.ceeol.com/search/article-detail?id=177994.
Kovács, F. (2011). Az alföldi területhasználat és változásainak értékelése [Evaluation of land use and its changes in the Great Hungarian Plain]. In J. Rakonczai (Ed.), Környezeti Változások és az Alföld [Environmental changes and the Great Hungarian Plain] (Vol. 7, pp. 159–166). Nagyalföld Alapítvány.
Lóczy, D., Éva, K., Schweitzer, F., 2009. Local flood hazards assessed from channel morphometry along the Tisza River in Hungary. Geomorphology 113 (3-4), 200–209. https://doi.org/10.1016/j.geomorph.2009.03.013.
Lunetta, R.S., Congalton, R.G., Fenstermaker, L.K., Jensen, J.R., McGwire, K.C., Tinney, L.R., 1991. Remote sensing and geographic information system data integration: error sources and research issues. Photogr. Eng. Remote Sens. 57 (6), 677–687. Retrieved from. https://www.asprs.org/wp-content/uploads/pers/1991journal/jun/1991_jun_677-687.pdf.
Linda, A.L., Geir, H.S., 2021. The content and accuracy of the CORINE Land Cover dataset for Norway. Int. J. Appl. Earth Observ. Geoinf. 96, 102266. https://doi.org/10.1016/j.jag.2020.102266.
Liu, Y., Meng, Q., Zhang, L., Wu, C., 2022. NDBSI: a normalized difference bare soil index for remote sensing to improve bare soil mapping accuracy in urban and rural areas. Catena (Amst) 214, 106265. https://doi.org/10.1016/j.catena.2022.106265.
Lyons, M.B., Keith, D.A., Phinn, S.R., Mason, T.J., Elith, J., 2018. A comparison of resampling methods for remote sensing classification and accuracy assessment. Remote Sens. Environ. 208, 145–153. https://doi.org/10.1016/j.rse.2018.02.026.
Lawrence, R.L., Wood, S.D., Sheley, R.L., 2006. Mapping invasive plants using hyperspectral imagery and Breiman Cutler classifications (randomForest) Remote Sens. Environ 100, 356–362. https://doi.org/10.1016/j.rse.2005.10.014.
Mohamed Abd, A., 2019. Land cover and land use classification performance of machine learning algorithms in a boreal landscape using Sentinel-2 data. GIsci. Remote Sens. 57 (1). https://doi.org/10.1080/15481603.2019.1650447.
Mudereri, B.T., Ayisi, K.K., Ramudzuli, M.R., 2023. A Systematic Review on Advancements in Remote Sensing for Assessing and Monitoring Land Use and Land

Cover Changes Impacts on Surface Water Resources in Semi-Arid Tropical Environments. Remote Sens. 15 (16), 3926. https://doi.org/10.3390/rs15163926.
Munthali, M.G., Davis, N., Adeola, A.M., Botai, J.O., Kamwi, J.M., Chisale, H.L.W., Orimoogunje, O.O.I., 2019. Local Perception of Drivers of Land-Use and Land-Cover Change Dynamics across Dedza District, Central Malawi Region. Sustainability. 11, 832. https://doi.org/10.3390/su11030832, 2019.
Molnár, E., Kozma, G., 2018. A debreceni gazdaságfejlesztés zászlóshajói: a városban működő ipari parkok jellegzetességei. (Flagships of economic development of Debrecen: characteristics of industrial parks in the city. Tér és Társadalom 33 (3), 49–71. https://doi.org/10.17649/TET.33.3.3188.
Matthews, F., Verstraeten, G., Borrelli, P., Panagos, P., 2022. A field parcel-oriented approach to evaluate the crop cover-management factor and time-distributed erosion risk in Europe. Int. Soil Water Conserv. Res. 11 (1), 43–59. https://doi.org/10.1016/j.iswcr.2022.09.005.
Monaghan, R.M., Laurenson, S., Dalley, D.E., Orchiston, T.S., 2017. Grazing strategies for reducing contaminant losses to water from forage crop fields grazed by cattle during winter. New Zealand J. Agric. Res. 60 (3), 333–348. https://doi.org/10.1080/00288233.2017.1345763.
Mengistu, T.D., Chung, I., Kim, M., Chang, S.W., Lee, J.E., 2022. Impacts and implications of land use land cover dynamics on groundwater recharge and surface runoff in East African watershed. Water. 14 (13), 2068. https://doi.org/10.3390/w14132068.
Martinez-Sanchez, L., See, L., Yordanov, M., Verhegghen, A., Elvekjaer, N., Muraro, D., d'Andrimont, R., van der Velde, M., 2024. Automatic classification of land cover from LUCAS in-situ landscape photos using semantic segmentation and a Random Forest model. Environ. Modell. Softw. 172, 105931. https://doi.org/10.1016/j.envsoft.2023.105931.
Moarrab, Y., Salehi, E., Amiri, M.J., et al., 2022. Spatial–temporal assessment and modeling of ecological security based on land-use/cover changes (case study: Lavasanat watershed). Int. J. Environ. Sci. Technol. 19 (11), 3991–4006. https://doi.org/10.1007/s13762-021-03534-5.
Maus, V., Câmara, G., Appel, M., Pebesma, E., 2019. dtwSat: time-weighted dynamic time warping for satellite image time series analysis in R. J. Stat. Softw. 88 (1), 1–3. https://doi.org/10.18637/jss.v088.i05.
Mountrakis, G., Im, J., Ogole, C., 2011. Support vector machines in remote sensing: A review. ISPRS J. Photogr. Remote Sens. 66 (3), 247–259. https://doi.org/10.1016/j.isprsjprs.2010.11.001.
Noi, P.T., Kappas, M., 2018. Comparison of Random Forest, k-Nearest Neighbor, and Support Vector Machine Classifiers for Land Cover Classification Using Sentinel-2 Imagery. Sensors 18 (1), 18. https://doi.org/10.3390/s18010018.
Nagy, A., Tamás, J., Burai, P., 2007. Application of advanced technologies for the detection of pollution migration. Cereal. Res. Commun. 35 (2), 805–809. https://doi.org/10.1556/CRC.35.2007.2.160.
I Nagy, A., Tamás, J., 2009. ntegrated airborne and field methods to characterize soil water regime. In: Celkova, A. (Ed.), Proceedings of peer-reviewed contributions, Transport of water, chemicals and energy in the soil-plant-atmosphere system. Institute of Hydrology. Slovak Academy of Sciences, Bratislava, pp. 412–420.
Nagy, A., Tamás, J., 2013. Noninvasive water stress assessment methods in orchards. Commun. Soil. Sci. Plant Anal. 44 (2), 366–376. https://doi.org/10.1080/00103624.2013.742308.
Navin, M.S., Agilandeeswari, L., 2020. Multispectral and hyperspectral images based land use /land cover change prediction analysis: an extensive review. Multimed. Tools. Appl. 79, 29751–29774. https://doi.org/10.1007/s11042-020-09531-z.
Nwagoum, C.S.K., Yemefack, M., Tedou, F.B.S., Fozing, T.T., 2023. Oben Sentinel-2 and Landsat-8 potentials for high-resolution mapping of the shifting agricultural landscape mosaic systems of southern Cameroon. Int. J. Appl. Earth. Obs. Geoinf. 124. https://doi.org/10.1016/j.jag.2023.103545.
Nguyen, V.S., Loisel, H., Vantrepotte, V., Mériaux, X., Tran, D.L., 2024. An empirical algorithm for estimating the absorption of colored dissolved organic matter from Sentinel-2 (MSI) and Landsat-8 (OLI) Observations of Coastal Waters. Remote Sens. 16 (21), 4061. https://doi.org/10.3390/rs16214061.
Njoku, E.A., Tenenbaum, D.E., 2022. Quantitative assessment of the relationship between land use/land cover (LULC), topographic elevation and land surface temperature (LST) in Ilorin. Nigeria. Remote Sens. Applic. Soc. Environ. 27, 100780. https://doi.org/10.1016/j.rsase.2022.100780.
Norovsuren, B., Tseveen, B., Batomunkuev, V., Renchin, T., Natsagdorj, E., Yangiv, A., Mart, Z., 2019. Land cover classification using maximum likelihood method (2000 and 2019) at Khandgait Valley in Mongolia. In: IOP Conference Series: Earth and Environmental Science, 381, 012054. https://doi.org/10.1088/1755-1315/381/1/012054.
Noble, W.S., 2006. What is a support vector machine? Nat. Biotechnol. 24 (12), 1565–1567. https://doi.org/10.1038/nbt1206-156.
Naesset, E., 1996. Conditional tau coefficient for assessment of producer's accuracy of classified remotely sensed data. ISPRS. J. Photogramm. Remote Sens. 51 (2), 91–98. https://doi.org/10.1016/0924-2716(69)00007-4.
Padma, S., Sanjeevi, S., 2014. Jeffries Matusita based mixed-measure for improved spectral matching in hyperspectral image analysis. Int. J. Appl. Earth Observ. Geoinf. 32, 138–151. https://doi.org/10.1016/j.jag.2014.04.001.
Pal, M., 2005. Random forest classifier for remote sensing classification. Int. J. Remote Sens. 26 (1), 217–222. https://doi.org/10.1080/01431160412331269698.
Pénzes, J., Hegedűs, L.D., Makhanov, K., Túri, Z., 2023. Changes in the patterns of population distribution and built-up areas of the rural–urban fringe in post-socialist context—A Central European case study. Land. (Basel) 12 (9), 1682. https://doi.org/10.3390/land12091682.
Pontius Jr, R.G., Millones, M., 2011. Death to kappa: birth of quantity disagreement and allocation disagreement for accuracy assessment. Int. J. Remote Sens. 32 (15), 4407–4429. https://doi.org/10.1080/01431161.2011.552923.
Pontius Jr, R.G., 2022. Metrics That Make a Difference: How to Analyze Change and Error. Springer Nature Switzerland AG, Switzerland. ISBN-10: 3030707644.
PROSPERA, 2020. Strategic Urban Development Strategy of Debrecen. Retrieved from projects2014-2020. https://projects2014-2020.interregeurope.eu/.
Petitjean, F., Kurtz, C., Passat, N., Gançarski, P., 2012. Spatio-temporal reasoning for the classification of satellite image time series. Pattern. Recognit. Lett. 33 (14), 1805–1815. https://doi.org/10.1016/j.patrec.2012.06.009.
Pal, M., Mather, P.M., 2003. Support vector classifiers for land cover classification. Map India 2003, Image Process. in-Terpretation. Retrieved from. http://www.gisdevelopment.net/technology/rs/pdf/23.pdf.
Qian, Y., Zhou, W., Yan, J., Li, W., Han, L., 2015. Comparing machine learning classifiers for object-based land cover classification using very high-resolution imagery. Remote Sens. 7 (1), 153–168. https://doi.org/10.3390/rs70100153.
Shetty, S., Gupta, P.K., Belgiu, M., Srivastav, S.K., 2021. Assessing the effect of training sampling design on the performance of machine learning classifiers for land cover mapping using multi-temporal remote sensing data and Google Earth Engine. Remote Sens. 13 (8), 1433. https://doi.org/10.3390/rs13081433.
Shi, F., Li, M., 2021. Assessing land cover and ecological quality changes under the new-type urbanization from multi-source remote sensing. Sustainability. 13 (21), 11979. https://doi.org/10.3390/su132111979.
Skidmore, A.K., Pettorelli, N., Tatem, A.J., Atkinson, P.M., 2021. Remote sensing for monitoring impacts of land-use change on biodiversity and carbon stocks. In Remote Sens. Monitor. Impacts Land-Use Change on Biodivers. Carbon Stocks - IIASA PURE.
Sim, W.D., Yim, J.S., Lee, J.S., 2024. Assessing Land Cover Classification Accuracy: Variations in Dataset Combinations and Deep Learning Models. Remote Sens. (Basel) 16 (14), 2623. https://doi.org/10.3390/rs16142623.
Settembre, G., Taggio, N., Del Buono, N., Esposito, F., Di Lauro, P., Aiello, A., 2024. A land cover change framework analyzing wildfire-affected areas in bitemporal PRISMA hyperspectral images. Math. Comput. Simul. 229, 855–866. https://doi.org/10.1016/j.matcom.2024.10.034.
Schoenbaum, I., Henkin, Z., Yehuda, Y., Voet, H., Kigel, J., 2018. Cattle foraging in Mediterranean oak woodlands: effects of management practices on the woody vegetation. For. Ecol. Manage 419–420 (2018), 160–169. https://doi.org/10.1016/j.foreco.2018.03.017.
Singh, M., Evans, D., Chevance, J., Tan, B.S., Wiggins, N., Kong, L., Sakhoeun, S., 2019. Evaluating remote sensing datasets and machine learning algorithms for mapping plantations and successional forests in Phnom Kulen National Park of Cambodia. Biodiversity and Conservation. Peer J. 7, e7841. https://doi.org/10.7717/peerj.7841.
Stehman, S.V., 2014. Estimating area and map accuracy for stratified random sampling when the strata are different from the map classes. Int. J. Remote Sens. 35 (17), 4923–4939. https://doi.org/10.1080/01431161.2014.930207.
STRATEGY 24 (2023): Debrecen fenntartható városfejlesztési stratégiája 2021–2027: Stratégiai munkarész. Hajdú-Bihar Megyei Közigazgatási Portál. Available online: https://hbmo.hu/portal/wp-content/uploads/2023/12/01B_eloterj.mell._DMJV-FVS-2021-27-strategiai-munkaresz.pdf.
Szász, G., 2013. Agrometeorological research and its results in Hungary (1870–2010). Q. J. Hungar. Meteorolog. Serv. 117 (3), 315–358. ISSN 03246329.
Szilassi, P., 2017. Magyarországi kistájak felszínborítás változékonysága és felszínborítás mozaikosságuk változása. Tájökológiai Lapok 15 (2), 131–138. https://doi.org/10.56617/tl.3612.
Tony, V.M.S., Jorge, R., 2022. On the quality of the drainage network cartographic representation. Ecol. Indic. 143. https://doi.org/10.1016/j.ecolind.2022.109350. Article 109350.
Tamás, J., Nagy, A., Buday-Bódi, E., Gálya, B., Nistor, S., Fehér, J., 2019. Guideline-Application of the Process Oriented Spatial Decision Support Tools: Methods in Urban Hydrology For Middle-Sized Cities in CEE Based on the Reference Sites. University of Debrecen, Debrecen, p. 93. University of Debrecen. Debrecen, 93.
Talukdar, S., Singha, P., Mahato, S., Shahfahad, Pal, S., Liou, Y.-A., Rahman, A., 2020. Land-use land-cover classification by machine. learning classifiers for satellite observations—a review. Remote Sens 12, 1135. https://doi.org/10.3390/rs12071135.
Teodoro, A.C., et al., 2024. Comparative study of random forest and support vector machine for land cover classification and post-wildfire change detection. Land. 13 (11), 1878. https://doi.org/10.3390/land13111878.
USGS, 2016. Earth Explorer. URL. https://earthexplorer.usgs.gov/.
Wiatkowska, B., Słodczyk, J., Stokowska, A., 2021. Spatial-temporal land use and land cover changes in urban areas using remote sensing images and GIS analysis: The case study of Opole. Poland. Geosci. 11 (8), 312. https://www.mdpi.com/2076-3263/11/8/312.
Williams, P., Biggs, J., Whitfield, M., Nicolet, P., Bray, S., Fox, G., Sear, D.A., 2004. Comparative biodiversity of rivers, streams, ditches and ponds in an agricultural landscape in Southern England. Biol. Conserv. 115 (2), 329–341. https://doi.org/10.1016/S0006-3207(03)00153-8.
Weng, Q., Lu, D., 2008. A sub-pixel analysis of urbanization effect on land surface temperature and its interplay with impervious surface and vegetation coverage in Indianapolis, United States. Int. J. Appl. Earth. Obs. Geoinf. 10 (1), 68–83. https://doi.org/10.1016/j.jag.2007.05.002.
Xie, Z., Chen, Y., Lu, D., Li, G., Chen, E., 2019. Classification of land cover, forest, and tree species classes with ZiYuan-3 multispectral and stereo data. Remote Sens. 11 (2), 164. https://doi.org/10.3390/rs11020164.

Yan, X., Li, J., Smith, A.R., Yang, D., Ma, T., Su, Y., 2023. Rapid land cover classification using a 36-year time series of multi-source remote sensing data. Land 12 (12), 2149. https://doi.org/10.3390/land12122149.

Yonaba, R., Koïta, M., Mounirou, L.A., Tazen, F., Queloz, P., Biaou, A.C., Niang, D., Zouré, C., Karambiri, H., Yacouba, H., 2021. Spatial and transient modelling of land use/land cover (LULC) dynamics in a Sahelian landscape under semi-arid climate in northern Burkina Faso. Land. Use Policy. 103. https://doi.org/10.1016/j.landusepol.2021.105305. Article 105305.

Zakariyya, I., Kalutarage, H., Al-Kadri, M.O., 2023. Towards a robust, effective and resource efficient machine learning technique for IoT security monitoring. Comput. Secur. 133, 103388. https://doi.org/10.1016/j.cose.2023.103388. ISSN 0167-4048.

Zhao, S., Tu, K., Ye, S., Tang, H., Hu, Y., Xie, C., 2023. Land use and land cover classification meets deep learning: a review. Sensors 23 (21), 8966. https://doi.org/10.3390/s23218966.

Zhang, T., Su, J., Xu, Z., Luo, Y., Li, J., 2021. Sentinel-2 satellite imagery for urban land cover classification by optimized random forest classifier. Appl. Sci. 11, 543. https://doi.org/10.3390/app11020543.